

DIPLOMARBEIT

Impedimetric biosensor for label-free multiplex detection of β -lactam antibiotic resistance genes employing Rolling Circle Amplification

Ausgeführt am Institut für

Chemische Technologien und Analytik (E164)

der Technischen Universität Wien

unter Anleitung von

Associate Prof. Mag.rer.nat Dr.rer.nat Martina Marchetti-Deschmann

In Kooperation mit

Dipl. Ing. Dr. Thomas Maier und Dipl. Ing. Dr. Rainer Hainberger

AIT – Austrian Institute of Technology GMBH, Department: Health & Environment

und

Dipl. Ing. Dr. Siegfried Krainer

Infineon Technologies Austria AG

durch

Kainz Konrad, BSc.

Andergasse 12/12/5, 1170 Wien

Wien, am

STATUTORY DECLARATION

I declare that I have authored this thesis independently, that I have not used other than the declared sources and that I have explicitly marked all material which has been quoted either literally or by content from the used sources.

Vienna,

.....

Konrad Kainz, BSc.

“A work as this is never finished,
one must simply declare it finished when one has,
within limits of time and circumstances,
done what is possible.”

Johann Wolfgang Goethe

(Iphigenie in Tauris, 1787)

Acknowledgements

First, I would like to thank my parents for their support in every way. Without their help it wouldn't have been possible for me to begin my studies in the first place, far less to complete them.

Furthermore, I would like to thank **Prof. Martina Marchetti-Deschmann**, who – as the supervisor of my bachelor thesis as well as of this master thesis – has given me the opportunity to write about this interesting topic.

A special thanks also goes to **Siegfried Krainer**, under whose supervision I already wrote my bachelor thesis at the AIT and who now made it possible for me to also do my master thesis at this company.

I also want to thank **Thomas Maier** for his great support concerning the physical problems and **Rainer Hainberger** and **all other colleagues at the AIT** for their support and help. A great thank you goes to **Ivan Barišić**, without his help concerning the biological aspects, this master thesis could not have been done so fast.

Finally I would like to thank all my friends who have given me support during the time of my studies and also while I was working on this thesis.

Thank you all, without every one of you this master thesis wouldn't exist.

Abstract

The aim of this work was the development and testing of an impedimetric based biosensor for the detection of antibiotic resistance genes using Rolling Circle Amplification (RCA) as the method of choice for isothermal amplification.

Before an own sensor ("Biosensor_RCA_bla_AIT") was developed, a biosensor ("Biosensor_Virus") provided by Infineon, Villach, was tested. This kind of system with interdigitated electrodes (IDEs) is normally used for another biological application, but initially it should be verified if this kind of sensor would also work in the case of the impedimetric detection of isothermal amplified deoxyribonucleic acid (DNA).

Because of the fast growing resistance to antibiotics by the extensive and very often unnecessary use in non-human fields, for instance in agriculture and the veterinary sector a rapid detection method is essential. The "golden" standard techniques for the detection of pathogens such as β -lactamases are based on cultivation methods in solid or liquid media. The advantages of disc diffusion tests or fully automated systems in clinical practice are that they are cheap and highly sensitive. But in some cases these methods are very time consuming: for instance the detection of mycobacterial growth, which can cause (among other diseases) tuberculosis, needs between four and eight weeks, which can be too long under some circumstances. Furthermore, potentially false-positive results are possible if the pathogens are exposed to wrong growing conditions.

With this newly developed biosensor it is possible to detect differences between positive DNA amplification and negative control. By a positive amplification reaction the impedance is changed over time to higher values whereas at a negative control stays the same or nearly the same. These differences in impedance are more pronounced at higher frequencies.

In this thesis it could be shown that the sensor is a potential candidate for the impedimetric detection of β -lactam antibiotic resistance genes especially if this system is modified to smaller sample volumes so that the cost-benefit relationship becomes more attractive. This modification process is also important in order to get lower target-DNA concentrations.

Now this system is able to detect $\sim 10^{12}$ molecules per milliliter, which is a very high DNA concentration that can only be reached by a pre-amplification step or the use of synthetic target-DNA.

Kurzfassung

Ziel dieser Arbeit war die Entwicklung und Prüfung eines auf Impedanz basierenden Biosensors für die Detektion von Antibiotikaresistenzgenen unter der Verwendung von einer isothermalen Amplifikation Methode, im speziellen Rolling Circle Amplification.

Bevor die Entwicklung eines eigenen Sensors, ("Biosensor_RCA_bla_AIT"), vorangetrieben wurde, sollte der Biosensor, ("Biosensor_Virus"), der Firma Infineon, Villach, getestet werden. Dieser Sensor, ausgestattet mit ineinandergreifenden Elektroden, wird für eine andere biologische Anwendung genutzt. Zu Beginn sollte jedoch überprüft werden, ob dieser Sensor ebenfalls für die Detektion von isothermal amplifizierter Desoxyribonukleinsäure (DNS) verwendet werden kann.

Wegen der sehr schnellen Zunahme von Antibiotikaresistenzen speziell durch den extensiven und sehr oft unnötigen Gebrauch von Antibiotika in nicht-menschlichen Bereichen, wie der Landwirtschaft und der Veterinärmedizin ist eine schnelle Detektionsmöglichkeit unumgänglich. Die Standardmethoden für die Detektion von Pathogenen basieren auf Kultivierungsmethoden in festen oder flüssigen Medien. Die Vorteile des Scheibendiffusionstest oder von vollautomatischen Systemen im klinischen Bereich sind vor allem die sehr günstigen Preise und die hohe Sensitivität. Allerdings sind diese Methoden teilweise sehr zeitaufwendig: Zum Beispiel kann die Detektion von Mykobakterien, welche unter anderem Tuberkulose auslösen können, vier bis acht Wochen dauern, was in einigen Fälle zu lange sein kann. Des Weiteren kann es zu falsch-positiven Resultaten kommen, wenn die Pathogene falschen Wachstumsbedingungen ausgesetzt werden.

Mit diesem neu entwickelten Biosensor ist es möglich, zwischen erfolgreicher und nicht erfolgreicher DNS-Vervielfältigung zu unterscheiden. Bei einer positiven Amplifikationsreaktion kommt es über die Zeit hinweg zu einer Erhöhung der Impedanzwerte, wohingegen das Messsignal bei einer negativen Kontrolle konstant bzw. nahezu konstant bleibt.

Im Laufe dieser Arbeit konnte gezeigt werden, dass dieser Sensor ein potentieller Kandidat für die impedimetrische Detektion von β -lactam Antibiotikaresistenzgenen sein kann, speziell, wenn dieses System zu kleineren Probenvolumina modifiziert wird, so dass der Kosten-Nutzenfaktor mehr an Bedeutung gewinnt. Dieser Modifikationsprozess ist ebenfalls notwendig, um zu niedrigeren DNS Konzentrationen zu gelangen.

Derzeit kann dieses System $\sim 10^{12}$ Moleküle pro Milliliter detektieren, was eine sehr hohe DNS Konzentration darstellt, welche nur durch eine Vorverstärkung oder durch die Verwendung von synthetischer DNS erreicht werden kann.

TABLE OF CONTENTS

1	<u>Introduction:</u>	- 1 -
1.1	<u>Antibiotics:</u>	- 1 -
1.1.1	<u>Definition of antibiotics:</u>	- 1 -
1.1.2	<u>Function of antibiotics:</u>	- 2 -
1.1.3	<u>Classes of antibiotics:</u>	- 3 -
1.1.3.1	<u>β-lactam antibiotics:</u>	- 3 -
1.1.3.2	<u>Tetracyclines:</u>	- 4 -
1.1.3.3	<u>Macrolide antibiotics:</u>	- 5 -
1.1.3.4	<u>Aminoglycosides:</u>	- 5 -
1.1.3.5	<u>Quinolones:</u>	- 6 -
1.1.3.6	<u>Glycopeptides:</u>	- 6 -
1.1.3.7	<u>Lincosamides:</u>	- 7 -
1.1.3.8	<u>Oxazolidinones:</u>	- 8 -
1.1.3.9	<u>Sulfonamides:</u>	- 8 -
1.1.4	<u>Antibiotic resistance:</u>	- 8 -
1.2	<u>β-lactamases:</u>	- 11 -
1.3	<u>DNA amplification methods:</u>	- 13 -
1.3.1	<u>Polymerase Chain Reaction:</u>	- 13 -
1.3.2	<u>Rolling Circle Amplification:</u>	- 16 -
1.4	<u>Impedance spectroscopy:</u>	- 20 -
1.4.1	<u>History:</u>	- 20 -
1.4.2	<u>Ohm's law:</u>	- 21 -
1.4.3	<u>Complex impedance:</u>	- 21 -
1.4.4	<u>Circuit Elements and their combinations:</u>	- 23 -

1.4.5	<u>Measurement of conductivity in liquids by impedance based measurements:</u>	25
2	<u>Material & Methods:</u>	30
2.1	<u>Equipment:</u>	30
2.2	<u>Chemicals:</u>	30
2.2.1	<u>General chemicals:</u>	30
2.2.2	<u>Phosphorylation:</u>	31
2.2.3	<u>DNA amplification:</u>	31
2.2.4	<u>Gel electrophoresis:</u>	31
2.2.5	<u>Programs:</u>	32
2.2.6	<u>Important parameters & informations:</u>	32
2.2.6.1	<u>LCR meter:</u>	32
2.2.6.1.1	<u>Frequency range:</u>	32
2.2.6.1.2	<u>Weakness of LCR meter:</u>	33
2.2.6.1.3	<u>Open-Short-correction:</u>	33
2.2.6.2	<u>Cleaning procedure - Biosensor RCA bla AIT:</u>	34
2.2.6.3	<u>Gel electrophoresis:</u>	34
2.2.6.4	<u>Biological system:</u>	35
2.3	<u>Rolling Circle Amplification:</u>	36
3	<u>Results & Discussion:</u>	40
3.1	<u>Biosensor Virus Infineon:</u>	40
3.2	<u>Biosensor RCA bla AIT:</u>	43
3.2.1	<u>Sensor setup and preliminary tests:</u>	43
3.2.1.1	<u>Electrodes with and without a glass separator in between:</u>	43
3.2.1.2	<u>Electrodes surrounded by glass capillaries:</u>	45
3.2.1.3	<u>The Influence of the filling levels and the number of glass layers:</u>	48

3.2.1.4	<u>The Influence of temperature:</u>	- 52 -
3.2.2	<u>Isothermal amplification:</u>	- 53 -
3.2.2.1	<u>Comparison of different amplification temperatures:</u>	- 57 -
3.2.2.2	<u>The Influence of different target-DNA concentrations:</u>	- 58 -
4	<u>Conclusion & Outlook:</u>	- 60 -
5	<u>References & Appendix:</u>	- 62 -
5.1	<u>List of references:</u>	- 62 -
5.2	<u>List of tables:</u>	- 67 -
5.3	<u>List of figures:</u>	- 67 -
5.4	<u>MATLAB - Source code of the $(R-2C_{\text{coupled}}) C_{\text{parasitic}}$ - ECM:</u>	- 70 -
6	<u>Curriculum Vitae:</u>	- 73 -

1 Introduction:

1.1 Antibiotics:

Nearly all physical methods, which are based on alcohol, 60-85 % of ethanol or ~70 % of isopropyl alcohol, cationic detergents, chlorine gas and so on, are too harsh or toxic to be used inside the human body or animals (or even for the treatment of plants) (Madigan *et al.* 2009).

For this reason chemical compounds (such as antibiotics) are required, which can be used for controlling infectious diseases inside the body (Madigan *et al.* 2009).

Without such compounds, thousands or millions of people would have died by various bacterial-induced diseases, such as tuberculosis and pest (Byarugaba 2010).

1.1.1 Definition of antibiotics:

Nowadays there exist many different definitions for the term "antibiotic". Each area, such as medicine, biology or pharmacy, has their own definition, but the main point of all these areas is that an antibiotic is any of various chemical substances, such as penicillin and streptomycin, which are produced by microorganisms, such as bacteria or fungi, that can harm or destroy the growth of other bacteria. Antibiotics are a subgroup of antimicrobials, which is a collective for anti-bacterials, anti-fungals, anti-protozoals and anti-virals, and are used to treat bacterial infections or to prevent infectious diseases. Antibiotics, which can be produced naturally, synthetically or semi-synthetically, can be divided into broad-spectrum, such as tetracyclines, which are against gram-positive and -negative bacteria, and narrow-spectrum antibiotics, such as penicillin, which is against gram-positive bacteria only (eMedExpert 2013; Zhang 2008).

Antibiotics, which had the nickname "wonder drug" during the Second World War, are one of the greatest inventions of the last millennium and were discovered by an "accident" more than 85 years ago by Alexander Fleming. In the year 1928 he observed the inhibition of growth of *Staphylococcus spp.* on agar plates, which were contaminated with other microorganisms. These microorganisms, later known as *Penicillium notatum*, were excreting some chemical compounds into the agar media, thereby causing an inhibition of bacterial growth. For this great discovery Fleming and two other guys, Chain and Florey, who worked on this topic in more detail later on, were awarded the Nobel Prize in Medicine in 1945 (Byarugaba 2010; Goddemeier 2006).

Today there are known thousands of antibiotics, but less than 1 % of these are clinically useful (Madigan *et al.* 2009).

Approximately 200 different antibiotics are produced by industry and more than half of them are semi-synthetic drugs, which leads to a decrease of toxicity and an increase of effectiveness since effectiveness and toxicity have an inverse relationship when you go from natural to semi- or fully-synthetic drugs (Schmid 2006; VITEK2 2008).

1.1.2 Function of antibiotics:

Antibiotics can exert their antimicrobial activity in two different ways.

On the one hand it works bactericidal, meaning that the microorganism is directly killed – examples are β -lactam antibiotics or cephalosporins – or on the other hand bacteriostatic, where the growth of a microorganism is inhibited – examples include tetracyclines or sulfonamides. It is important to know that there is not always a highly accurate difference between bactericidal and bacteriostatic antibiotics. A low concentration of some bactericidal antibiotics causes bacteriostatic and vice versa.

The reason why antibiotics work by bacterial cells, also called prokaryotic cells, and not by human and other eukaryotic cells is that there are some differences in the cellular architecture of these two types. Prokaryotic cells are smaller than eukaryotic ones, and they do not have a nucleus. Moreover, the cell division is by binary fission whereas in eukaryotic cells mitosis or meiosis is the main reproduction way. The weight of the ribosomes is also different, in prokaryotic cells they are smaller (70S) than in eukaryotic ones (80S) (Bendich and Drlica 2000; Rollins 2004).

There are five ways how bacteriostatic agents work, see figure 1 (Madigan *et al.* 2009; Byarugaba 2010):

- a) Interferences with cell wall synthesis
- b) Inhibition of protein synthesis
- c) Inhibition of synthesis of essential metabolites
- d) Injury to cytoplasmic membrane structure and function
- e) Interferences with nucleic acid replication and transcription

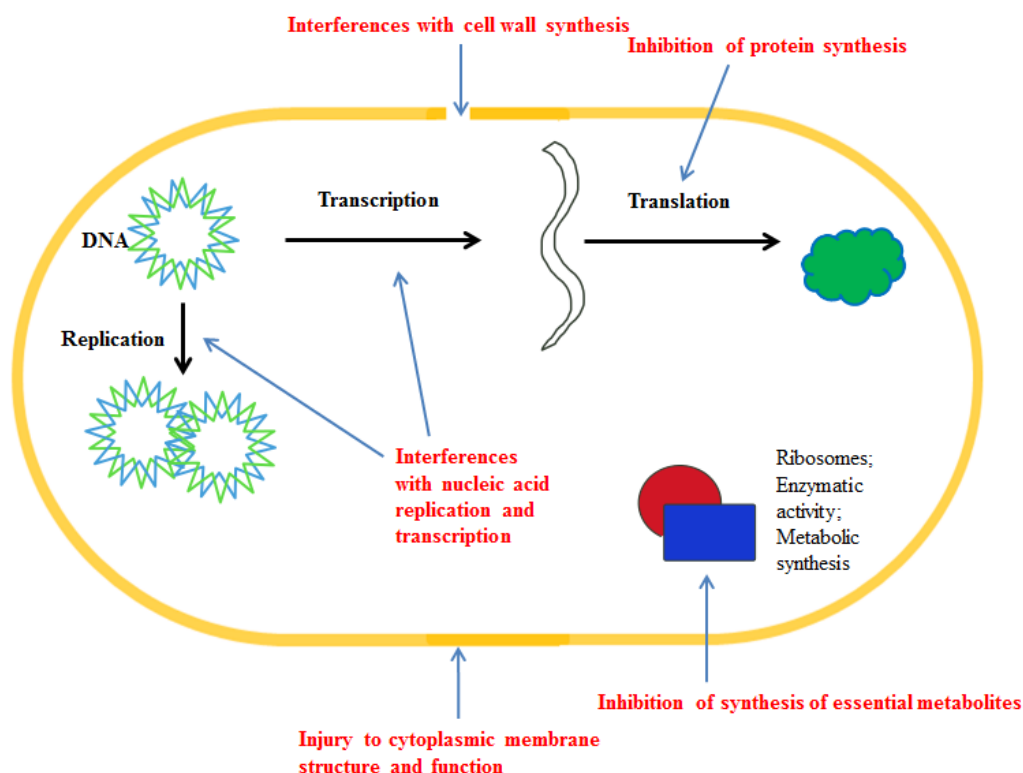


Figure 1: Illustration of a microbial cell. Five major modes of action of bacteriostatic antibiotics.

1.1.3 Classes of antibiotics:

Antibiotics are divided into different classes, depending on the target site and mechanism of action (Madigan *et al.* 2009).

1.1.3.1 β -lactam antibiotics:

β -lactam antibiotics or β -lactams are among the world's most important antibiotics. About 50 % of the estimated global market is contributed to β -lactams, which is more than 16 billion dollars (Schmid 2006). Today there are ~50 different kinds of β -lactams available on the market (VITEK2 2008).

They bind covalently and irreversibly to the penicillin-binding-protein (PBP), which is responsible for the formation of peptide bonds in the bacterial cell wall component peptidoglycan. When penicillin binds to such a PBP-region, the cell is not able to catalyze the transpeptidase reaction anymore, but the cell wall synthesis still continues. This leads to a new synthesized cell wall, which is no longer cross-linked within each other and as a result of this, the osmotic pressure differences between inside and outside the cell cause lysis, which leads to the death of the cell (Walsh 2000).

β -lactams are highly selective and not toxic to host cells because of the unique cell wall structure of bacteria, which is different from eukaryotic cells so that antibiotics cannot harm humans or animals. The differences between these two types of cells are described in chapter 1.1.2.

Penicillin – mechanism of action (Yusof *et al.* 2011):

The β -lactam mimics the Acyl-D-Ala-D-Ala structure, which is responsible for cross-linking and binds to the transpeptidase, the enzyme which has the function to link the peptidoglycan molecules to each other. This leads to weakness of the cell wall when the bacterium divides. An illustration of this mechanism is shown in figure 2.

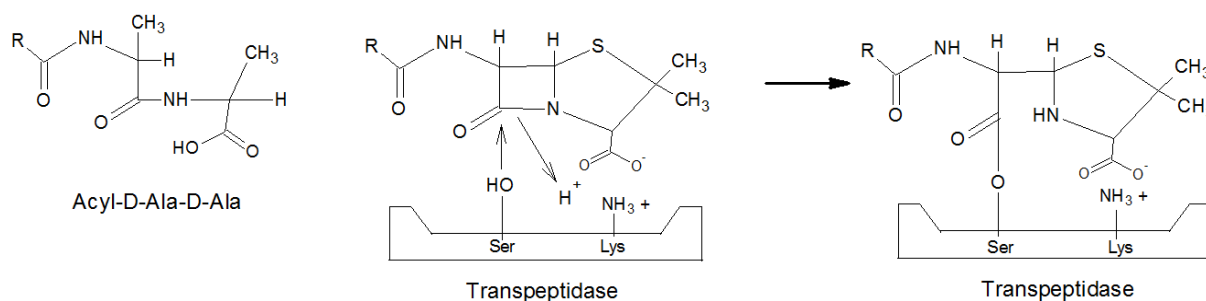


Figure 2: Penicillin mechanism of action. The penicillin imitates the Acyl-D-Ala-D-Ala structure and inhibits so the growth of the bacterial cell.

1.1.3.2 Tetracyclines:

Tetracyclines are, after β -lactams, the second important group of antibiotics inhibiting nearly all gram-negative and -positive bacteria. Tetracyclines consist of a naphthacene ring system and inhibit the protein synthesis by the accretion of aminoacyl-t-Ribosenucleic acid (RNA) to the 30S subunit of the ribosomes, thus inhibiting the elongation of peptide-chain (Budkevich *et al.* 2008; Madigan *et al.* 2009).

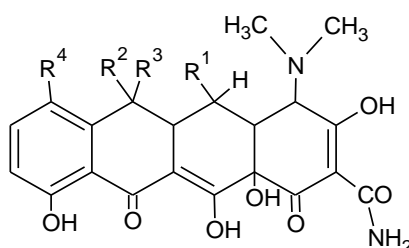


Figure 3: Analogs of tetracycline. Different substitutes of R^1 - R^4 see table 1.

Table 1 lists some analogs of tetracycline antibiotics.

Table 1: Semi-synthetic analogs of tetracycline antibiotics (Madigan *et al.* 2009). Residue (R).

	R ¹	R ²	R ³	R ⁴
Tetracycline	H	OH	CH ₃	H
7-Chlortetracycline (aureomycin)	H	OH	CH ₃	Cl
5-Oxytetracycline (terramycin)	OH	OH	CH ₃	H

1.1.3.3 Macrolide antibiotics:

The production of macrolide antibiotics covers ~11 % of the world's total requirement of antibiotics. They consist of large lactone rings to which deoxy sugars are bonded. Because of the great variation in both the lactone rings and deoxy sugars this kind of antibiotic has a large number of representatives. Macrolide antibiotics, which are broad-spectrum antibiotics, bind reversible to the 50S subunit of the bacterial ribosome and so inhibit the protein synthesis (Madigan *et al.* 2009; Schmid 2006).

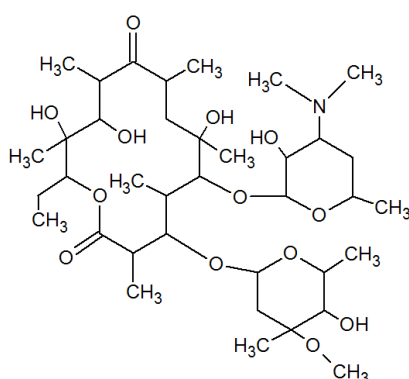


Figure 4: Illustration of erythromycin. One macrolide ring combined with two deoxy sugars.

1.1.3.4 Aminoglycosides:

Aminoglycosides are antibiotics in which amino sugars bonded together by glycosidic linkage. They are clinically useful against gram-negative bacteria, such as *Yersinia pestis* and also gram-positive aerobes, such as *Mycobacterium tuberculosis*, and target the 30S subunit of the bacterial ribosome and so inhibit protein synthesis (Schmid 2006).

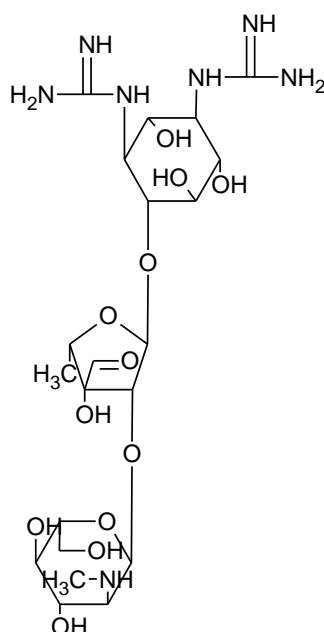


Figure 5: Illustration of Streptomycin, which was discovered by Selman Waksman in the year 1943.

1.1.3.5 Quinolones:

Quinolones interfere with the replication step and so prevent the supercoiling of deoxyribonucleic acid (DNA), an important step before packing DNA into the bacterial cell, by disruption of the enzyme, DNA gyrase.

An important example is Ciprofloxacin, which is the medicine of choice when treating an anthrax infection as some strains of *Bacillus anthracis* are resistant against penicillin (Hooper 1999; Madigan *et al.* 2009).

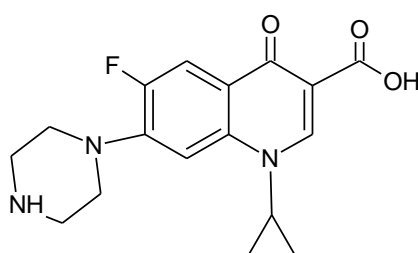


Figure 6: Illustration of ciprofloxacin. It is a fluorinated derivate of nalidixic acid and reaches therapeutic levels in tissues and also in blood.

1.1.3.6 Glycopeptides:

Glycopeptides such as vancomycin bind directly to the terminal D-alanyl-D-alanine peptide on the peptidoglycan precursor and interfere so with cell wall synthesis. This leads to a

blocking of the transpeptidation, the cross-linking reaction of two glycan-linked peptide chains (Van Bambeke *et al.* 2004).

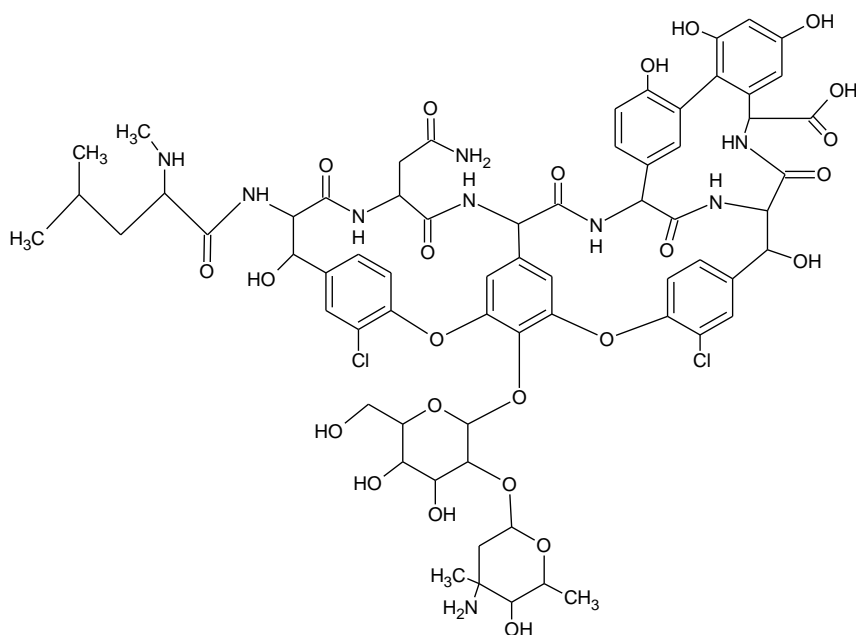


Figure 7: Illustration of vancomycin used in the treatment of gram-positive bacterial infection, first isolated from Eli Lilly in the year 1953.

1.1.3.7 Lincosamides:

Lincosamides interfere with protein synthesis and so they prevent bacterial replication. In detail this kind of antibiotic binds to the 23S region of the 50S subunit of bacterial ribosomes and this leads to premature dissociation of the peptidyl-tRNA (Tenson *et al.* 2003).

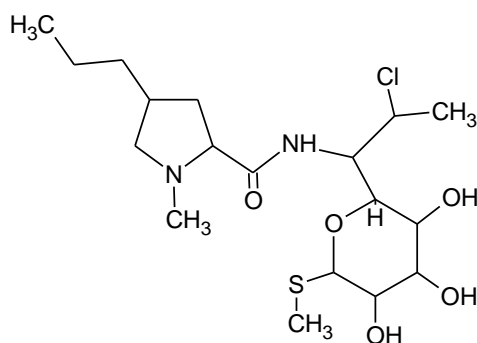


Figure 8: Illustration of clindamycin used in the treatment of anaerobic bacterial infection or protozoal diseases, such as malaria.

1.1.3.8 Oxazolidinones:

Oxazolidinone antibiotics bind to the 50S subunit ribosome and inhibit bacterial protein synthesis through inhibition of formation of the 70S initiation complex (Diekema and Jones 2001).

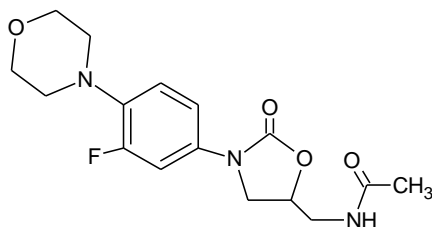


Figure 9: Illustration of linezolid, also called zyvox. It is used in the treatment of serious infections and was first discovered in the 1990s.

1.1.3.9 Sulfonamides:

Sulfonamides were the first antibiotics and led to a revolution in medicine. Prontosil, discovered in 1932, was the first representative of this antibiotic group that could treat some bacterial infections. Sulfonamides inhibit the enzyme dihydropteroate synthase (DHPS), which is involved in the synthesis of essential metabolites (Ruggy 1945).

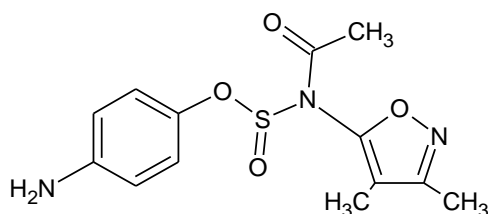


Figure 10: Illustration of sulfisoxazole, also known as sulfafurazole. It is used in the treatment of gram-positive and -negative bacteria.

1.1.4 Antibiotic resistance:

By the extensive use of antimicrobial agents, such as in clinical practice or nonhuman regions, bacterial resistance is increasing more and more.

Some reasons for increasing antibiotic resistances are, inter alia, the following (Aarestrup *et al.* 2001; Byarugaba 2004, 2010; Giedraitiene *et al.* 2011):

- use of antimicrobial agents for prophylaxis
- suboptimal treatment of infections

- increasing numbers and durations of hospital stays which are often unnecessary
- increasing travel
- use of antibiotics in agriculture and the veterinary area

To control the spread of antimicrobial resistant bacteria, all of these points must be addressed. Bacterial resistance to antimicrobial agents such as antibiotics can be described in two different ways:

- intrinsic or innate, which depends on the biology of a microorganism, such as gram-negative or -positive bacteria. For example *Escherichia coli* has a natural resistance to vancomycin (Giedraitiene *et al.* 2011). That means that a microorganism does not possess a target site for a special chemical compound and so this compound does not harm or kill the microorganism or they have low permeability to these compounds because of the differences in their chemical structure.
- acquired resistance whereby microorganisms find some ways to not be affected by an antimicrobial agent. An example for this process is the modification of the target site where glycopeptides, such as vancomycin, work. By changing the normal D-Ala-D-Ala structure to D-Ala-D-Lac at the C-terminus, vancomycin cannot bind anymore or at least not so well, which leads to an affinity of vancomycin for this new terminus which is 1,000 times lower (Dzidic *et al.* 2008).

The acquired resistance mechanism occurs in different ways. The overview below lists the main types of biochemical mechanisms that are used by bacteria to defend themselves against antibiotics (Byarugaba 2010; Fluit *et al.* 2001):

- inactivation of the microbial agent through the presence of a specific enzyme
- existence of an alternative enzyme, a microbial agent or alternative mechanism for an enzyme which is inhibited and was previously unknown
- modification of the target region through mutation, which leads to a reduction of the binding probability of an antimicrobial agent
- modification of the transcription or translation region, which leads to a reduced binding probability
- efflux whereby microorganism may be able to pump out antibiotics

- reducing of the antimicrobial agent concentration through overproduction of the specific target

Two different ways to genetically encode antibiotic resistance of a microorganism either on the chromosome or on a plasmid called R-plasmid, whereas R stands for resistance, are known (Madigan *et al.* 2009).

Many different reasons for the genetics of antibiotic resistance are known today, such as spontaneous mutation, horizontal gene transfer, etc.

Spontaneous or chromosomal mutations are mutations without external causes, such as the proton tunneling in DNA (Löwdin 1963), and are quite rare. For instance, only one microorganism in a population of 10^6 - 10^8 is normally mutated (Giedraitiene *et al.* 2011). The causes of these mutations are errors in the replication cycle on the one hand, and incorrect repair of damaged DNA on the other. As an example, quinolone resistance in *Escherichia coli* is caused by changes of only three amino acids in the *parC* gene or in at least seven amino acids in the *gyrA* gene (Dzidic *et al.* 2008; Hooper 1999).

Adaptive mutation is a theory which goes against the traditional theory of evolution. This kind of theory states that mutations are not being random, but are in response to specific stress, such as temperature changes, population size and nutrients. (Cairns *et al.* 1988).

Another mechanism is horizontal gene transfer (HGT), also termed lateral gene transfer (LGT), which is the primary reason for antibiotic resistance of bacteria (Kay *et al.* 2002; Koonin *et al.* 2001). Today there are known several mechanisms, such as transformation, transduction and bacterial conjugation (Giedraitiene *et al.* 2011; Griffiths *et al.* 2000; Todar 2009).

1.2 β -lactamases:

β -lactam antibiotics form the most important group of antibiotics of the world. As previously explained in more detail in chapter 1.1.3.1 they bind covalently to the PBP, thereby inhibiting the formation of the peptide bonds inside the bacterial cell wall.

β -lactam antibiotics are effective against both gram-positive and -negative bacteria. For this reason it is of immense significance, especially for clinical use, if bacteria are resistant to this class of antibiotics (Kiiru *et al.* 2012). Today and particularly in the future, antimicrobial resistance is and will be a growing problem. *Enterobacteriaceae*, such as *Escherichia coli* or *Klebsiella pneumoniae*, are the primary causes of diseases worldwide and β -lactam antibiotics, such as cephalosporin, are the best way to treat this kind of infections. For instance, *Klebsiella pneumoniae* is a pathogen which causes urinary tract infections (Nasehi *et al.* 2010) and some serotypes of *Escherichia coli* are responsible for infections of the intestine, such as diarrhea as well as urinary tract infections and neonatal meningitis (Clermont *et al.* 2000).

The enzymes that protect a microorganism against β -lactam antibiotics are called β -lactamases. For instance, through the hydrolysis of the β -lactam-bond the function of the antibiotic is disturbed and so they do not harm the bacterial cell anymore. This process is the most common mechanism of resistance (Bush and Jacoby 2010; Walther-Rasmussen and Hoiby 2007). The resistance to these drugs due to β -lactamases is considered one of the most important reasons. Today more than 300 different enzymes which inactivate β -lactam antibiotics are known (Majiduddin *et al.* 2002).

The β -lactamases can be classified into two different schemes:

- The Ambler classification (1980)
- The Bush-Jacoby-Medeiros classification (1995)

The Ambler molecular scheme divides β -lactamases into four different groups, based on their amino acid sequences, labeled A, B, C and D, whereby classes A, C and D are based on a serine mechanism and class B on metallo- β -lactamase, which needs zinc in order to function (Kong *et al.* 2010; Walther-Rasmussen and Hoiby 2006, 2007). The Bush-Jacoby-Medeiros classification divides β -lactamases by their functional similarities and distinguishes between four groups and different subgroups (Bush *et al.* 1995; Paterson and Bonomo 2005).

Table 2 shows an overview about the 33 most important clinical β -lactamases and their classification, which depends on the sequence similarity.

For these 33 different β -lactamases 96 padlock probes were designed to detect special regions of the genes. The target sequences, padlock probes, etc. are available at the dissertation of Ivan Barišić, more details see chapter 2.2.6.4.

Table 2: 33 Important clinical β -lactamases. Their classification is based on their sequence similarity (Classification by Ambler). The padlock probes were designed to detect the different genes. It is not possible to distinguish between ESBL-TEM and SHV and NSBL-TEM and SHV because no probes were made for Single-Nucleotide-Polymorphism-(SNP)-Detection.

	Class A	Class B	Class C	Class D
ESBLs	CTX-M-1			
	CTX-M-2			
	CTX-M-8			
	CTX-M-9			
	CTX-M-25			
	GES-1			
	PER-1			
	RTG-4			
	SFO-1			
	VEB-1			
Carbapenemases	IMI-1	IMP-1		OXA-23
	KPC-1	IMP-24		OXA-24
	SME-1	VIM-1		OXA-48
		VIM-2		OXA-51
		NDM-1		OXA-58
AmpCs			ACT-1	
			CMY-1	
			CMY-2	
			DHA-1	
			FOX-1	
			MIR-1	
NSBLs	SHV-1			OXA-1
	TEM-1			OXA-2

1.3 DNA amplification methods:

1.3.1 Polymerase Chain Reaction:

The Polymerase Chain Reaction (PCR) is the most common and best investigated method of DNA amplification. It was developed by Kary Mullis and his coworkers in the mid 1980s, who received the Nobel Prize in Chemistry for this invention in 1993 (Saiki *et al.* 1985).

PCR is designed for a special gene fragment, called target, of a template DNA, which is much larger than the target. The template is either single-stranded (ss)- or double-stranded (ds)-DNA or RNA. Furthermore, the PCR needs two oligonucleotide primers, called forward- and reverse-primer, that flank the DNA template to be amplified and serve as a starting region for the DNA-polymerase, such as *Taq-polymerase* (isolated from the bacteria *Thermus aquaticus*) or *Pfu-polymerase* (isolated from the archaeobacteria *Pyrococcus furiosus*). The PCR also requires deoxynucleoside triphosphates (dNTPs), which are a mixture of deoxyadenosine (dATP), deoxycytidine (dCTP), deoxyguanosine (dGTP) and deoxythymidine triphosphate (dTTP), magnesium sulfate, for a better ionic transport, and a polymerase buffer.

The whole PCR process can be divided into 3 steps which are repeated several times (~30 cycles) (Kubista *et al.* 2006). Figure 11 shows an illustration of the PCR mechanism (see page 15).

a) Denaturation of the DNA strain:

At this step a high temperature, around 95 °C, is applied to the system to separate DNA strands from each other. This separation is also called melting. In this process the hydrogen bonds of the DNA are split up, whereby adenosine and thymidine have a double bond and cytosine and guanosine a triple bond. Often it is also necessary to denature for several minutes at the beginning to activate the polymerase – such polymerases are called Hotstart-polymerase.

b) Annealing of the two oligonucleotide primer:

Then the temperature is lowered to 50-60 °C depending on the primer sequence, so that the primers can anneal to the template. The annealing temperature shall be ~5 °C below the melting temperature of these two primers. If it is too high there will be a low PCR yield because of the insufficient primer-template hybridization. If it is too low this can lead to non-specific primer-template binding and thus to false DNA products (Rychlik *et al.* 1990).

The optimal annealing temperature (T_a^{OPT}) can be calculated with the empirical formulation below (Rychlik *et al.* 1990):

$$T_a^{OPT} = 0.3 * T_M^{Primer} + 0.7 * T_M^{Product} - 14.9$$

T_M^{Primer} melting temperature of the less stable primer-template pair.

$T_M^{Product}$ melting temperature of the PCR product.

The melting temperature of the primer (T_M^{Primer}) can be calculated as follows (Rychlik *et al.* 1990):

$$T_M^{Primer} = \frac{\Delta H}{\Delta S * R * \ln\left(\frac{c}{4}\right)} - 273.15 + 16.6 * \log [K^+]$$

ΔH enthalpy for helix formation

ΔS entropy for helix formation

R molar gas constant ($8.31446 \text{ m}^2\text{kg}\cdot\text{s}^{-2}\cdot\text{K}^{-1}\cdot\text{mol}^{-1}$)

c total molar concentration of the annealing primer

K^+ molar concentration of potassium - correction term because PCR is conducted in 50 mM K^+

The melting temperature of the product ($T_M^{Product}$) can be calculated as follows (Rychlik *et al.* 1990):

$$T_M^{Product} = 0.41 * (\% G + \% C) + 16.6 * \log[K^+] - \frac{675}{l}$$

l length of the product in nucleotide (nt) residues

K^+ molar concentration of potassium - correction term because PCR is conducted in 50 mM K^+

$\% G$ percentage of guanosine

$\% C$ percentage of cytosine

c) Amplification, Elongation or Extension of the DNA strand:

In analogy to the replication of DNA in the nucleus, the DNA-polymerase synthesizes the missing strand of the ss-DNA with nucleotides. The optimum working temperature depends on the used polymerase. In case of *Taq-polymerase* it is about 70 °C and the rate of DNA amplification is about 50-100 nt per second (Maloy 2002).

The “standard” PCR consists of two primers and is an exponential amplification method. After 31 temperature cycles there is a multiplication of the gene fragment, starting with 1 DNA fragment, by a factor of 2^{30} , which is equivalent to ~1 billion copies.

Another PCR method is the so called linear-PCR, where only one oligonucleotide primer is used instead of two. This leads to a linear growth of DNA concentration. Starting with 1 DNA template and assuming 2000 copies per minute and an amplification time of 1 hour this leads to 120.000 copies, much less than in “standard”, exponential PCR.

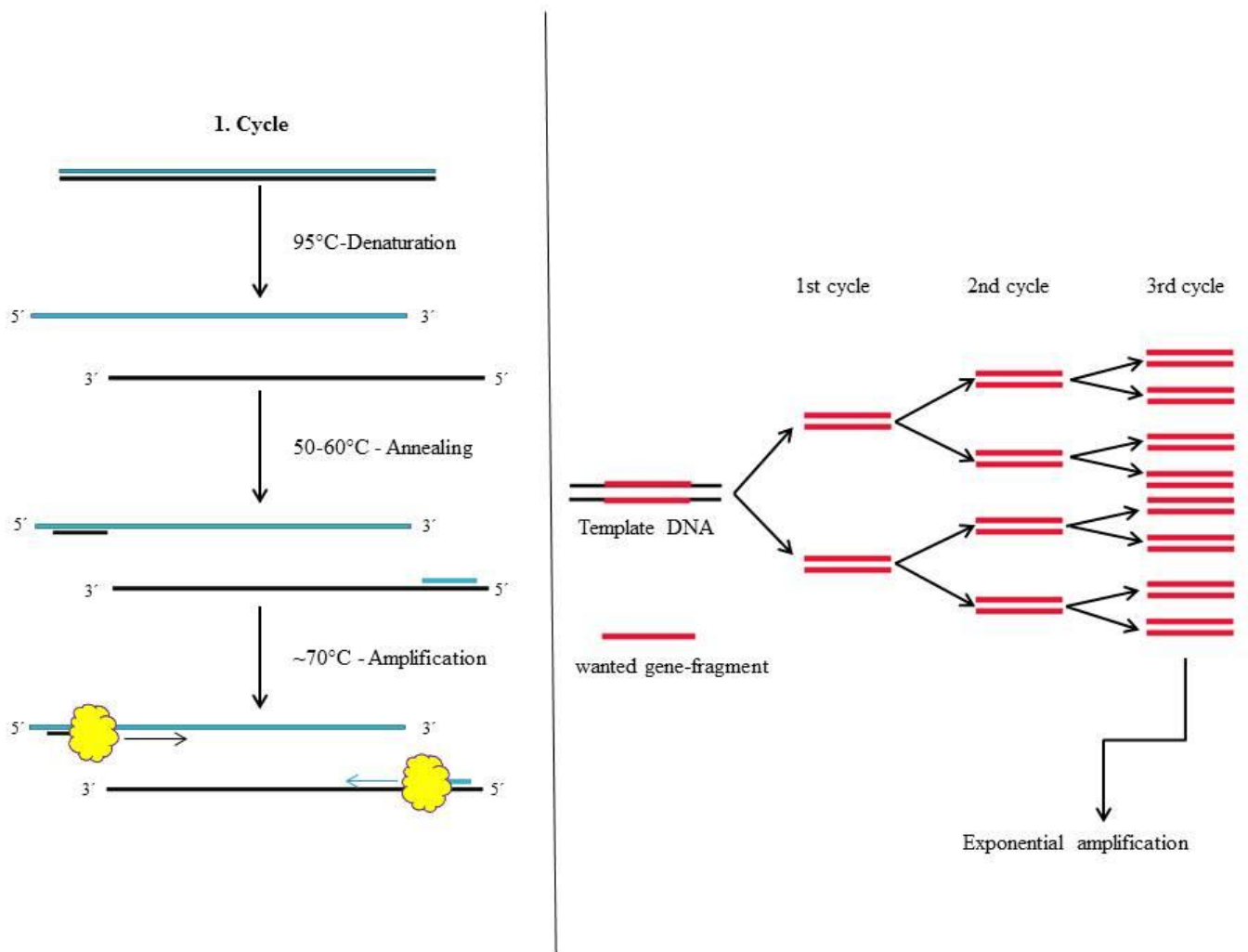


Figure 11: Mechanism of PCR. Left side: Overview of one cycle, consisting of three different sequential steps; Step 1: Denaturation of DNA; Step 2: Primer annealing; Step 3: Amplification/Elongation/Extension of DNA. Right side: Overview about the exponential growth rate, using “standard” PCR.

1.3.2 Rolling Circle Amplification:

Rolling Circle Amplification (RCA) or Rolling Circle Replication (RCR) is one of several known isothermal amplification methods such as loop-mediated isothermal amplification (LAMP), helicase-dependent amplification (HDA), isothermal multiple displacement amplification (IMDA), recombinase polymerase amplification (RPA), nucleic acid sequence-based amplification (NASBA), etc. (Gill and Ghaemi 2008; Zanolli and Spoto 2013).

In comparison to PCR, described in chapter 1.3.1, isothermal amplification methods do not need a thermal cycler to operate which leads to a minimization of costs especially for lab-on-a-chip devices (Zanolli and Spoto 2013). Another advantage of RCA in combination with padlock probes is that it is resistant to contamination (Mothershed and Whitney 2006).

Because of the special ability of the polymerase to displacing the DNA strand, the amplification can take place under isothermal conditions. Today several polymerases with this strand-displacing character are known, such as BST-polymerase (isolated from the bacteria *Bacillus stearothermophilus*) or phi29 DNA-polymerase (isolated from the bacteria *Bacillus subtilis* phage $\phi 29$). The main difference of these two polymerases is the working temperature. In the case of BST-polymerase the amplification temperature should be $\sim 60^\circ\text{C}$ and the phi29 DNA-polymerase has its optimum working temperature at 37°C .

So far two different RCAs have been developed. One is the linear RCA, where a little circle sequence is amplified by a complementary primer, the other is the exponential RCA, which works with two primers. In the exponential case the second primer hybridize with the ss-DNA product of the first primer and initiates hyper-branching in the DNA-replication (Mothershed and Whitney 2006).

Padlock Probes are linear oligonucleotides that consist of various specific regions and enable a much higher degree of multiplexing than multiplex-PCR (Barišić *et al.* 2013; Nilsson *et al.* 2006). Figure 12 shows an overview of the four different elements on one padlock probe. Every padlock probe consists of a unique barcode sequence for microarray hybridization, a circle-to-circle-amplification sequence (C2CA) and a 5' and 3' target-DNA recognition sequence.

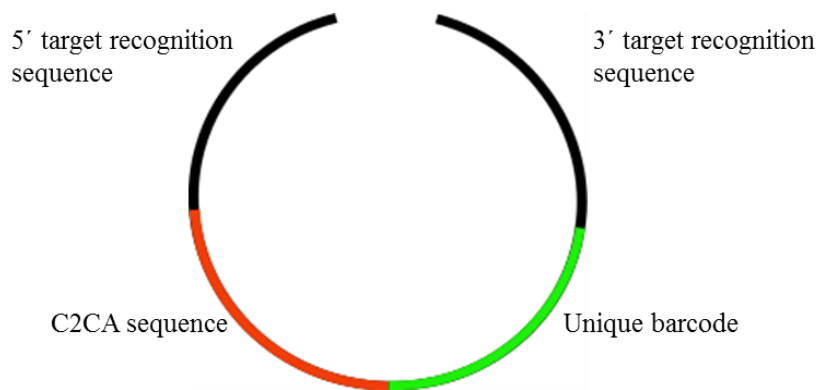


Figure 12: Schematic illustration of the four different elements on a padlock probe. Each padlock probe consists of an unique barcode for microarray hybridization, a C2CA sequence and the two target-DNA recognition sequences.

After the hybridization of the padlock probe head-to-tail onto the target-DNA, the nick which was formed between the two ends is recognized and afterwards sealed by a DNA ligase. Figure 13 illustrates this process. On the left side a positive ligation step is shown, when padlock probe and target-DNA fit perfectly together so that the DNA ligase is able to close the resulting nick. On the right side the result of a negative ligation process is displayed, where the two DNA pieces do not completely match so that there is no ligation.

The so circularized probes serve as a template for the following RCA reaction. After the ligation step the complementary C2CA-primer hybridizes onto the padlock probe and works as a starting point for the phi29 DNA-polymerase that synthesizes the new ss-DNA strand, consisting of repetitive sequences of the padlock probes (Andras *et al.* 2001).

Because of the unique target recognition sequences and consequently low probability to cross-reactions, padlock probes are very suitable for multiplex detection.

When the very efficient phi29 DNA-polymerase is used, it is possible to achieve a billion-fold amplification, assuming that three cycles of C2CA and ~1000 monomers are produced within a RCA of one hour (Nilsson *et al.* 2006).

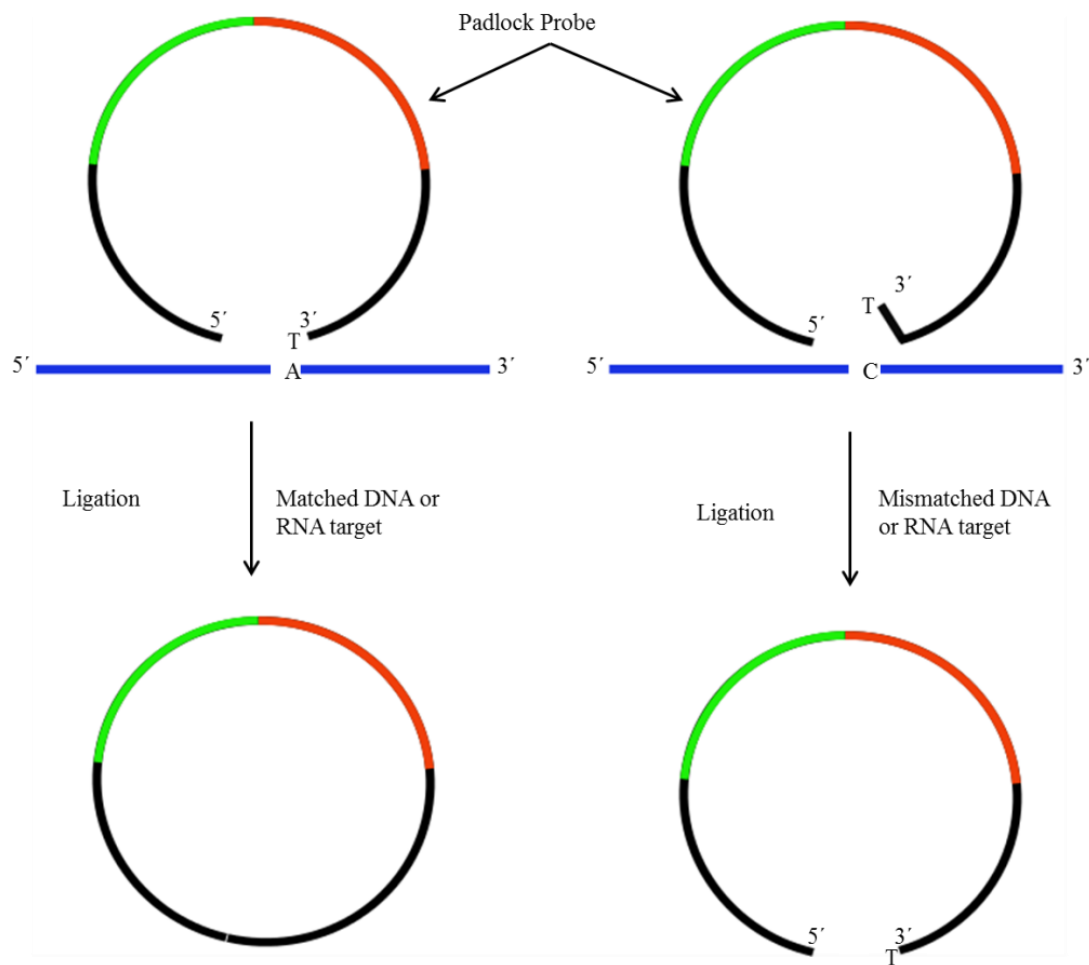


Figure 13: Schematic illustration of padlock probes through ligation process. On the left side the result of a positive ligation step is represented, when target-DNA and padlock probe absolutely fit together, and on the right side it can be seen what happens if these two DNA fragments do not fit together, which leads to no circularization of the padlock probe.

The mechanism of the used RCA is shown in figure 14 and consists of the following steps:

a) Hybridization and Ligation:

By this procedure the target-DNA hybridizes onto the padlock probe and the so formed nick is closed by the use of a DNA ligase if both sequences (target-DNA and padlock probe) fit perfectly together. This process is described in more detail above (figure 13).

b) 1st RCA cycle:

By using of the complementary C2CA-primer, which hybridizes onto the ligated padlock probe, the sequence of this circularized padlock probe is amplified resulting in a long ss-DNA.

c) Digestion (Monomerization and Ligation):

The RCA product, which is now single-stranded, gets incubated with C2CA-oligonucleotides which have an internal restriction site that allows them to monomerize the RCA-products with the special restriction enzyme *AluI*.

d) 2nd RCA cycle:

After the digestion another RCA cycle is done, whereas ligation of the previously synthesized DNA and new amplification step are done at the same time, under the use of a special DNA ligase, so called T4-DNA ligase.

e) Linear PCR (optional step):

In this optional step the new synthesized ss-DNA can be labeled with a fluorophore for microarray hybridization. In contrast to a “normal”, exponential PCR, which works with two primers, in the linear PCR only one primer is added, which leads to ss-DNA.

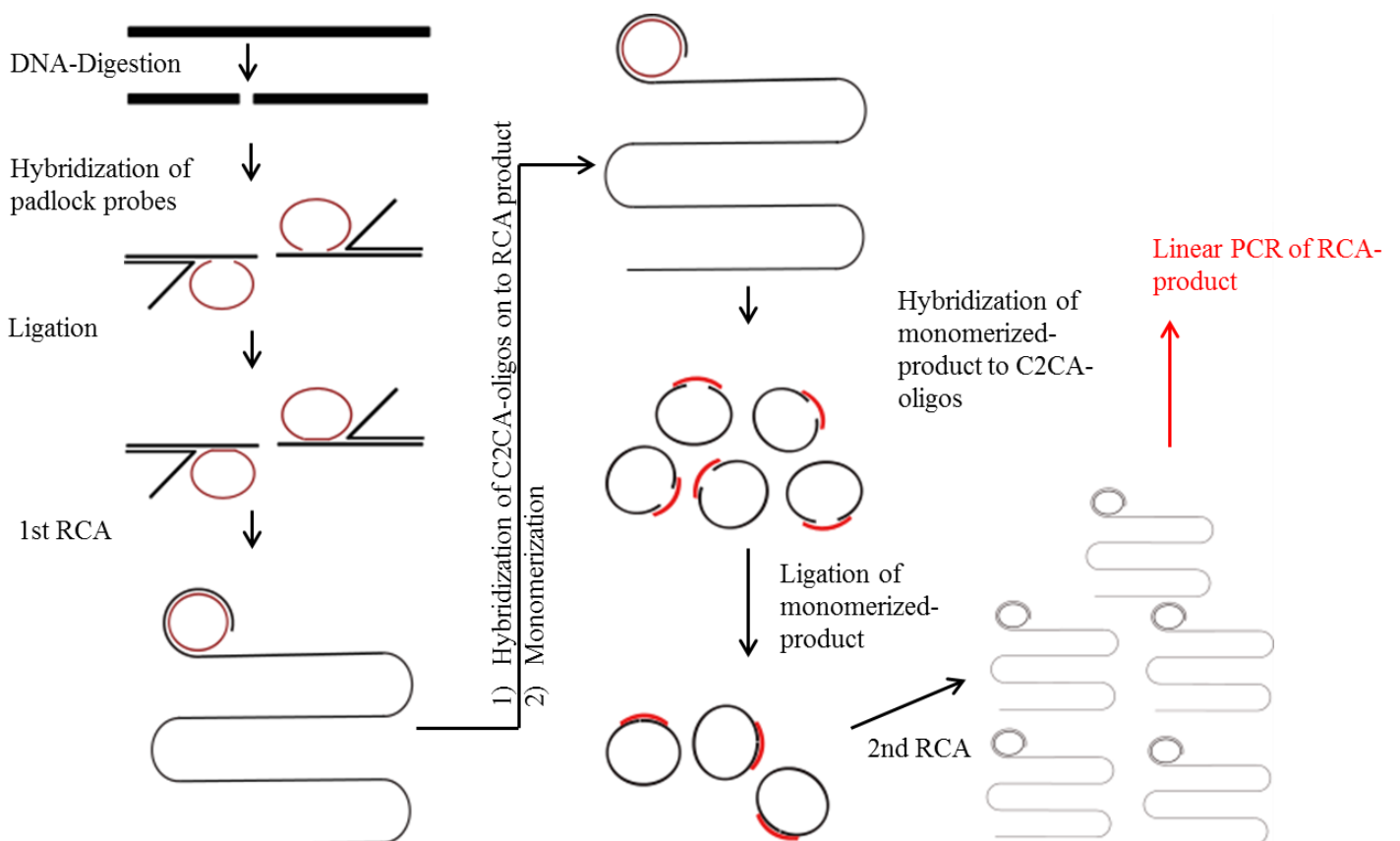


Figure 14: Mechanism of RCA/RCA. Step 1: Hybridization and Ligation of the padlock probes; Step 2: 1st RCA cycle; Step 3: Digestion of RCA product; Step 4: 2nd RCA cycle combined with ligation mechanism; Step 5 (optional step): labeling of the ss-DNA to use it for the hybridization on a microarray.

1.4 Impedance spectroscopy:

Impedance Spectroscopy (IS), also known as Dielectric Spectroscopy, is a powerful and new analytical tool with a tremendous increase in popularity in the last few decades.

In this technique, a sinusoidal excitation voltage is applied to an electrode-probe-system which usually consists of a network of different electric components, like resistors, capacitances or inductances. The relation between excitation voltage and the current through the electrode-probe-system, including the phase shift between voltage and current – the so called impedance – is measured. The frequency dependence of the impedance – the impedance spectrum – allows the identification of the different electrical components in the system and the measurement of their individual properties.

This "simple" concept is also one of the most important reasons why this technique became so popular in applied chemistry. Today this analytical technique is used to a huge number of different important areas, such as:

- label-free biosensors (Daniels and Pourmand 2007; Ertuğrul and Uygun 2013)
- corrosion (Hamdy *et al.* 2006)
- fuel cells (Gomadam and Weidner 2005)
- conducting polymers (Inzelt 2007)
- and many other applications (Barsoukov and Macdonald 2005; Lvovich 2012)

1.4.1 History:

With the introduction of complex quantities and especially the operational calculus in the 1880s by Oliver Heaviside, the successful history of IS begins. After this, A.E. Kennelly and C.P. Steinmetz included vector diagrams and complex representations, which leads to another step in the evolution of IS. The next milestone for the analysis of real systems was done by Cole and Cole (1941) by plotting ϵ' (x or real axis) against ϵ'' (y or imaginary axis), which is now known as Cole-Cole plot. Complex plane plots are often also called Nyquist diagrams, where the real part is plotted against the imaginary one.

Because of the availability of new, faster and more sensitive equipment since the late 1960s IS has become more and more attractive. Since 1993 the Chemical Abstract database shows ~1500 citations per year including the term "impedance". In the earlier years this number has

slightly decreased to ~1200 citations per year, but the term “impedance” may also include non-electrochemical impedance experiments (Lasia 1999).

1.4.2 Ohm's law:

The electrical resistance, R , of a circuit element describes its ability to transport an electrical current. Ohm's law defines the resistance of an object as the ratio of the voltage and the electrical current:

$$R = \frac{E}{I}$$

R ... resistance of an object [Ω]

E ... voltage across an object [V]

I ... electrical current, which goes through an object [A]

Historically, Ohm's law was formulated for constant currents and voltages. To describe the relation between time dependent currents and voltages, the so called Impedance, Z , is introduced. In analogy to Ohm's law it is defined as:

$$Z = \frac{E}{I}$$

1.4.3 Complex impedance:

A monochromatic sinusoidal voltage

$$E_t = E_0 \sin(\omega t)$$

where E_t is the potential at time t , E_0 is the amplitude of the signal, and ω ($\omega = 2 * \pi * f$) is the radial frequency, is applied to a cell, which leads to the resulting alternating current

$$I_t = I_0 \sin(\omega t + \theta)$$

Here, θ is the phase shift between the applied voltage signal and the resulting current. It describes the time lag between voltage and current, see figure 15 (Gamry 2010).

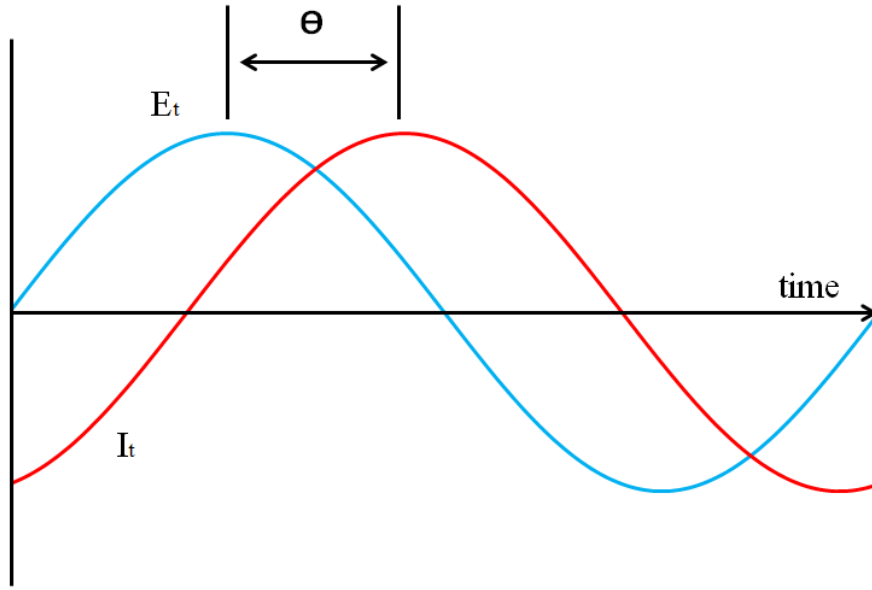


Figure 15: Sinusoidal current response in a linear system. Phase shift between applied sinusoidal voltage E_t and resulting alternating current I_t can be observed.

In analogy to Ohm's law the impedance is defined as:

$$Z(j\omega) = Z(\omega) = \frac{E(j\omega)}{I(j\omega)}$$

where $j \equiv i = \sqrt{-1}$.

Z is a complex number and can be expressed as a vector in a rectangular coordinate system. The real part of Z , $\text{Re}(Z)$, is in the direction of the horizontal real-axis and the imaginary part of Z , $\text{Im}(Z)$, belongs to the vertical imaginary axis, as shown in figure 16.

$$Z(\omega) = \text{Re}(Z(\omega)) + j * \text{Im}(Z(\omega))$$

Using Euler's relation

$$\exp(j\theta) = \cos(\theta) + j * \sin(\theta)$$

it is possible to represent Z in polar coordinates:

$$Z(\omega) = |Z(\omega)| * \exp(j\theta)$$

where $|Z(\omega)|$ is the absolute value of Z and phase, θ is the phase angle (See figure 16).

$$|Z(\omega)| = \sqrt{(\text{Re}(\omega))^2 + (\text{Im}(\omega))^2}$$

$$\theta = \arctan\left(\frac{\text{Im}(\omega)}{\text{Re}(\omega)}\right)$$

$$\text{Re}(Z(\omega)) = |Z(\omega)| * \cos(\theta)$$

$$\text{Im}(Z(\omega)) = |Z(\omega)| * \sin(\theta)$$

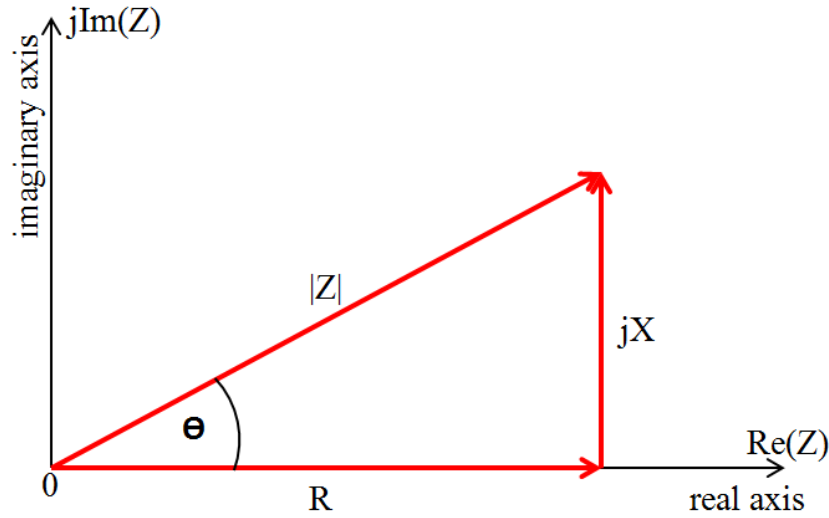


Figure 16: The impedance plotted using rectangular and polar coordinates.

1.4.4 Circuit Elements and their combinations:

In simple cases, the investigated electrode-probe-system can be modeled using common electrical elements such as capacitors, C, inductors, L, and resistors, R (Lvovich 2012). Table 3 represents an overview of the AC characteristics of these elements. More sophisticated models may include Warburg impedances (induced by diffusion processes) or constant phase elements (CPE) (models the behavior of a non-ideal capacitor).

Table 3: Common electrical circuit elements.

Component	I vs. E	Z	Phase shift
Capacitor [F, or ohm ⁻¹ *s]	$I = C * \frac{dE}{dt}$	$Z = \frac{1}{j * \omega * C}$	- 90 degree
Inductor [H, or ohm*s]	$E = L * \frac{di}{dt}$	$Z = j * \omega * C$	+ 90 degree
Resistor [ohm]	$E = I * R$	$Z = R$	Stays in phase

The impedance of a capacitor decreases with increasing frequencies, its real part is zero, its imaginary part is negative.

The impedance of an inductor increases with increasing frequencies, its real part is zero, its imaginary part is positive.

The impedance of a resistor is not influenced by the frequency, its real part is positive, its imaginary part is zero.

The behavior of the different electrical circuit elements builds the fundamentals of the impedance spectroscopy.

An electrode-probe-system is represented by an equivalent circuit model (ECM). Such a model consists of a network of several different impedances, which can be combined in series or parallel (Figure 17). Applying Kirchhoff's laws, one obtains easily the two relations given below.

In case of elements, which are connected in series to each other, the total impedance can be calculated according to:

$$Z_{total} = Z1 + Z2 + Z3 \quad \rightarrow \quad Z_{total} = \sum_{i=1}^n Z_i$$

In case of elements, which are connected in parallel to each other, the total impedance can be calculated according to:

$$\frac{1}{Z_{total}} = \frac{1}{Z1} + \frac{1}{Z2} + \frac{1}{Z3} \quad \rightarrow \quad Z_{total} = \frac{1}{\sum_{i=1}^n \frac{1}{Z_i}}$$

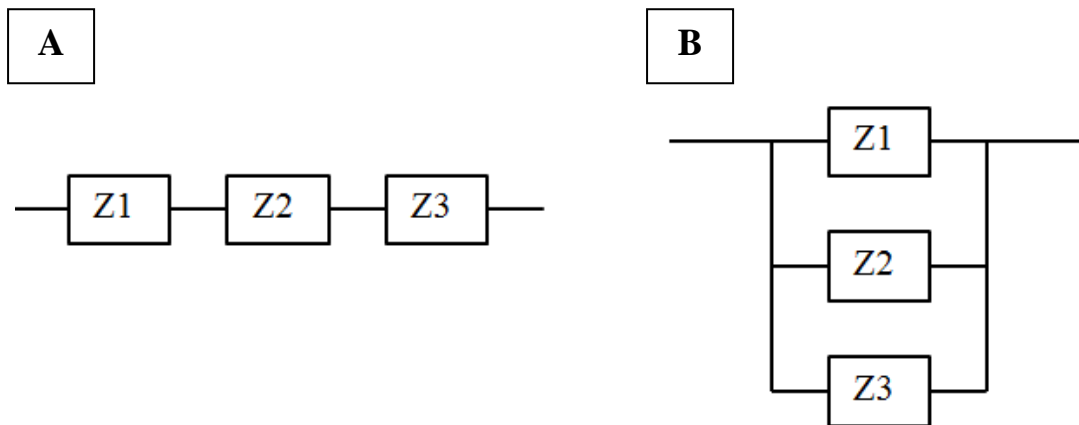


Figure 17: (A) Impedance in series and (B) in parallel.

1.4.5 Measurement of conductivity in liquids by impedance based measurements:

An illustration of a simple ECM for the sensors investigated in this thesis, is shown in figure 18. A resistor (R-Analyte) represents the conductivity of the liquid to be measured. The electrodes are not in direct contact with the liquid. They are covered by a thin, insulating passivation layer, represented by $C_{coupled}$.

The use of passivated electrodes has some advantages, such as:

- no corrosion process could take place
- better reproducibility of the measurements
- no electrochemical processes in the surrounding medium

Another capacitance ($C_{parasitic}$) describes the dielectric coupling between the two electrodes. Depending on the actual sensor geometry, $C_{parasitic}$ is a network of capacitances involving the capacitance of the liquid, $C_{coupled}$, and the dielectric crosstalk across the substrate (in the case of thin film sensors, like the Biosensor_Virus provided by Infineon, described in more detail in chapter 3.1).

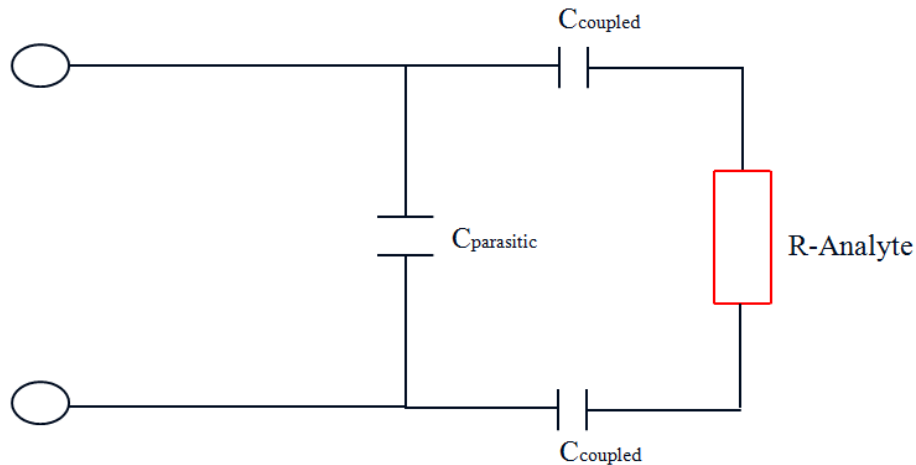


Figure 18: Simplified ECM consisting of a resistor in series with two coupling capacitances ($R-2C_{coupled}$) and this whole circuit is parallel to the parasitic capacity $[(R-2C_{coupled})||C_{parasitic}]$.

Using equations (network of parallel and series impedance elements, described in chapter 1.4.4), the total impedance of this circuit can be calculated. The circuit is separated into two parts:

- Circuit I:

This circuit element consists of the resistor in series with two coupling capacitances ($R - 2C_{coupled}$).

$$Z_I = R - Analyte + 2 * \frac{1}{j * \omega * C_{coupled}} = R - Analyte + \frac{1}{j * \pi * f * C_{coupled}}$$

- Circuit II:

This circuit consists of the circuit I in parallel with the parasitic capacity $[(R - 2C_{coupled}) || C_{parasitic}]$.

$$\begin{aligned} Z_{total} &= \frac{Z_I * \frac{1}{j * \omega * C_{parasitic}}}{Z_I + \frac{1}{j * \omega * C_{parasitic}}} = \\ &= \frac{\left(R - Analyte + \frac{1}{j * \pi * f * C_{coupled}} \right) * \frac{1}{j * \omega * C_{parasitic}}}{\left(R - Analyte + \frac{1}{j * \pi * f * C_{coupled}} \right) + \frac{1}{j * \omega * C_{parasitic}}} \end{aligned}$$

Z_{total} represents the impedance of the whole system. Here the real and imaginary part are not separated from each other. The equations above were entered in MATLAB (code see chapter 5.4) and the impedances were calculated for three different resistances ($R - Analyte$).

Impedance spectra of these calculations are shown in figure 19. For a first, qualitative discussion, the results are shown in arbitrary units. On the low frequency side, the impedance is entirely dominated by the coupling capacity. As the impedance of a capacity is inversely proportional to the frequency, the frequency dependence is given by a falling straight line in the log-log scale of figure 19. As the frequency increases, the impedance of $C_{coupled}$ decreases further, until it becomes smaller than $R - Analyte$. In this frequency range, the total impedance is dominated by the value of $R - Analyte$. Shoulders appear in the spectrum, where the impedance is almost frequency-independent, and the spectra for the different values of $R - Analyte$ clearly split up. Note that the shoulder shifts to higher frequencies for smaller values of $R - Analyte$. Finally, at high frequencies, the impedance of $C_{parasitic}$ becomes smaller than $R - Analyte$. Just like for low frequencies, the impedance is independent of $R - Analyte$ again.

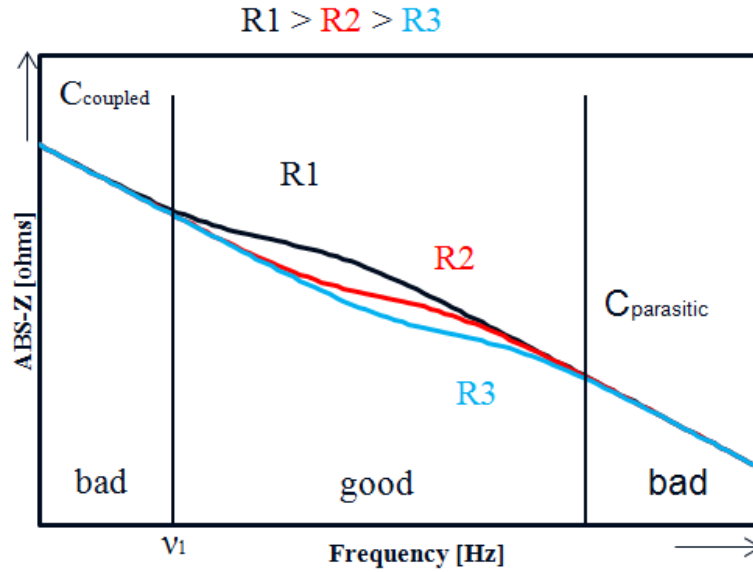


Figure 19: LOG-LOG representation of ABS-Z vs. frequency for three different values of R-Analyte ($R1 > R2 > R3$).

Bearing in mind, that the maximum frequency of instruments for impedance spectroscopy are limited usually around 1 MHz, these findings make clear, that the choice of proper values for $C_{coupled}$ and R-Analyte in the sensor design is substantial for the proper operation of the sensor.

Figure 20 represents calculations for a coupling capacity of 6 nanofarad (nF), a parasitic capacity of 200 picofarad (pF) and a resistance value of 10 kOhm, illustrating the frequency dependencies on ABS-Z, phase, real and imaginary part. As the imaginary part is negative, the absolute value is plotted.

Real part would be best for the determination of R-Analyte because it assumes the value of R-Analyte until high frequencies than parasitic capacity dominates. The value of R-Analyte is also observable on the plateau or shoulder of ABS-Z. The phase also reflects the previously discussed frequency dependence: At low frequencies the phase is close to -90° (coupling capacity dominates), as well as high frequencies (parasitic capacity dominates), in between the phase approaches to 0° , which reflects the increasing ohmic resistance in the total impedance.

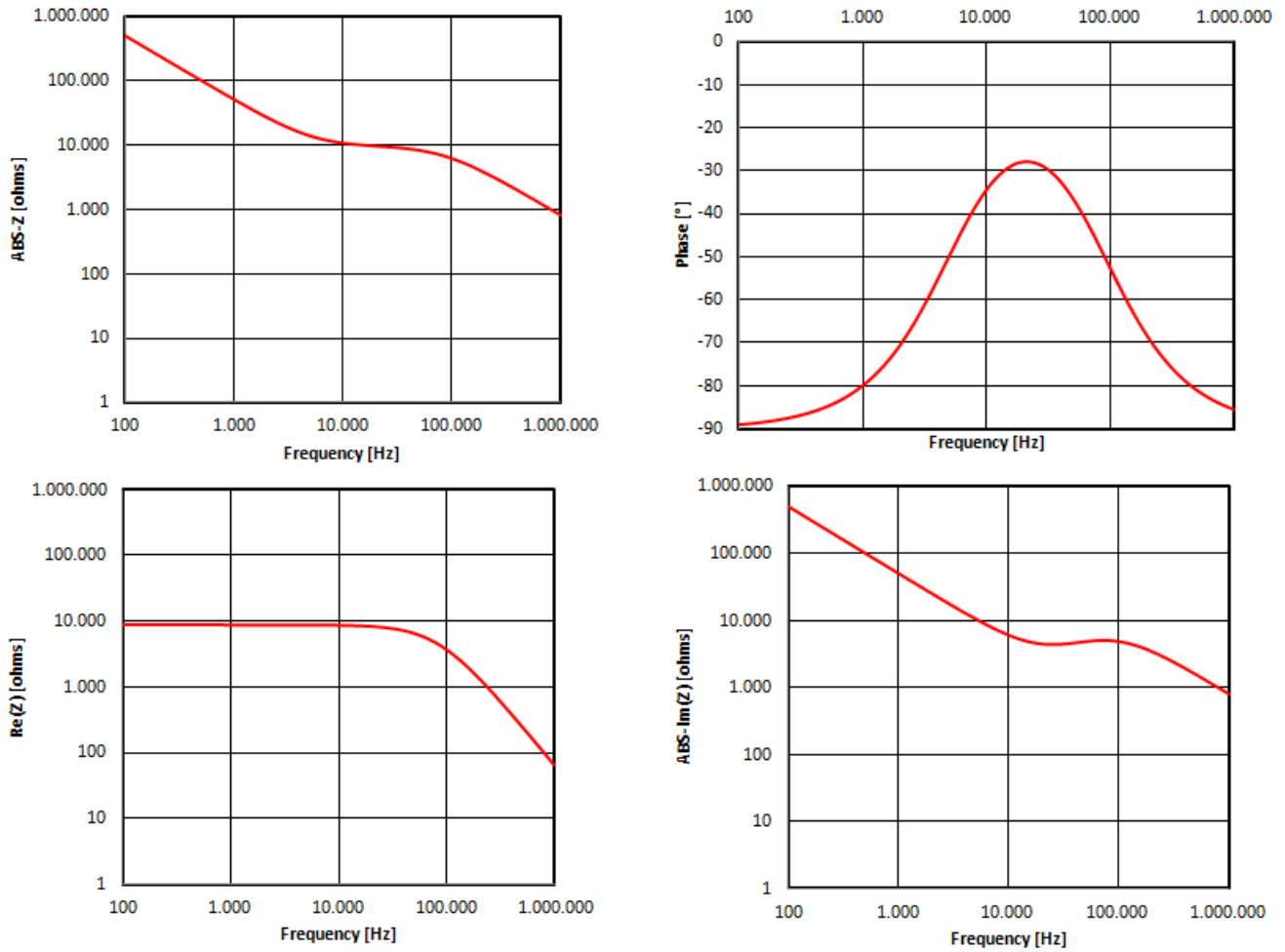


Figure 20: ABS-Z, phase, Re(Z) and ABS-Im(Z) for $C_{\text{coupled}} = 6 \text{ nF}$, $C_{\text{parasitic}} = 200 \text{ pF}$ and $R_{\text{Analyte}} = 10 \text{ kOhm}$ vs. frequency (100 Hz - 1 MHz).

Figure 21 represents calculations for four different parasitic capacitances (100, 200, 800 and 1600 pF) and three different coupling capacitances (3, 6 and 18 nF) illustrating the frequency dependencies of ABS-Z and resulting phase. The resistance value amounted 10 kOhm at all four calculations.

The halving of both the coupling and parasitic capacitances from 6 nF respectively 200 pF (red solid line) to 3 nF and 100 pF (red dashed line) leads to a shift of the phase maximum to higher frequencies. Also the ABS-Z is shifted in parallel direction to higher values.

An unequal change of both capacitances to higher values from $C_{\text{coupled}} = 6 \text{ nF}$ to 18 nF and $C_{\text{parasitic}} = 200 \text{ pF}$ to 800 pF (red solid line in comparison to black solid line) induces a phase shift to lower frequencies and to lower values of the phase maximum.

By this variation also the ABS-Z values at the beginning and the end are influenced, but also the plateau.

A doubling of the parasitic capacitance to higher values at constant coupling capacity, 800 pF to 1600 pF, (black solid line vs. black dashed line) leads first, to a minimization of the phase maximum and second, to a shrinking of the plateau at ABS-Z.

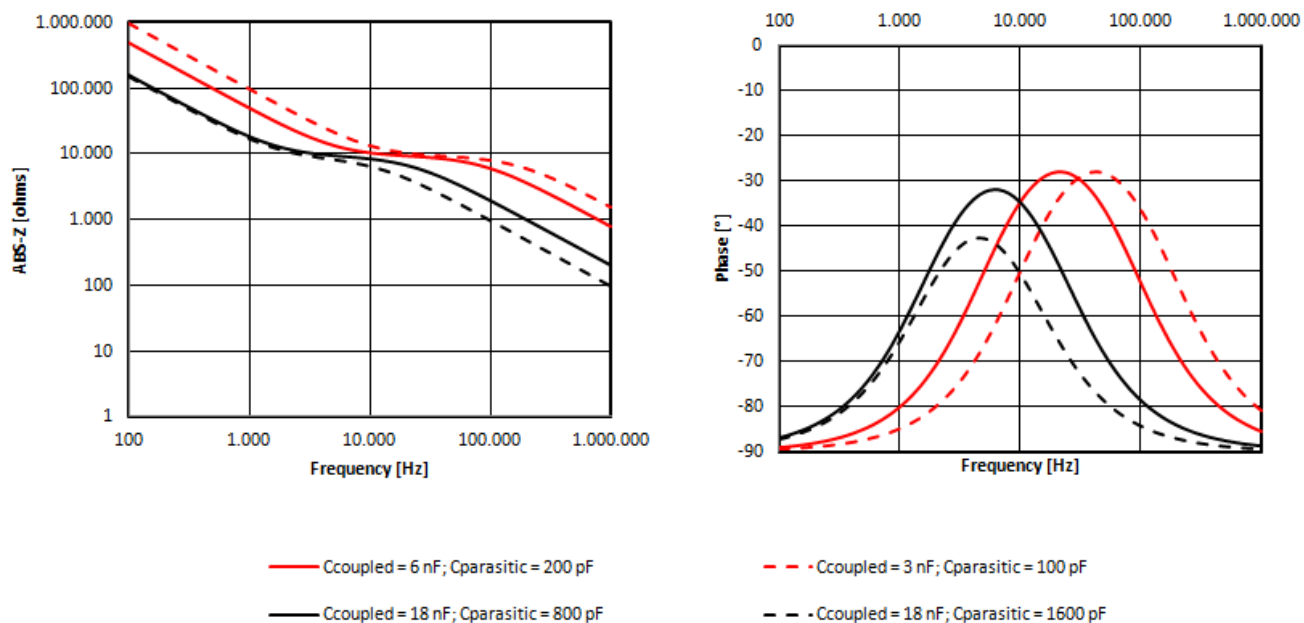


Figure 21: ABS-Z and phase for different coupling and parasitic capacitances at a value of $R_{\text{Analyte}} = 10 \text{ kOhm}$ vs. frequency (100 Hz - 1 MHz). A change of coupling and/or parasitic capacitances are observable best at the resulting phase.

2 Material & Methods:

2.1 Equipment:

Biosensor Virus Infineon:

The biosensors (see figure 23) are provided by Infineon, Villach. This system should be tested if it is usable for molecular diagnostic.

Biosensor RCA bla AIT:

Self-developed biosensor for detection of isothermal amplified DNA (1st RCA cycle). At figure 28 the final sensor (A) and a schematic overview (B) are visible. bla is a synonym for β -lactamase.

LCR meter:

“HP 4248A Precision Semiconductor Parameter Analyzer” (Agilent Technologies) was controlled by a personal computer using LabView for operation. The LCR meter is a highly accurate machine for electronic device characterization, whereas L stands for inductance, C for capacitance and R for resistance.

PCR-Cycler:

“GeneAmp[®] PCR System 2700” (Applied Biosystems, CA 94404, USA) was used for the ligation step and also for the further amplification of DNA (Digestion and 2nd RCA step).

UV-Imaging System:

“Bio-Spectrum[®] Imaging System – Model BioSpectrum 310” (UVP, CA 91786, USA) is a fully automated system for research. This UV-imaging system was used to control the DNA amplification after the 2nd RCA cycle.

2.2 Chemicals:

2.2.1 General chemicals:

Deionized water (dH₂O):

18.2 MOhm; Evoqua Water Technologies, Siemens.

Potassium chloride (KCl):

P3911-1KG; Sigma Aldrich, Vienna, Austria.

2.2.2 Phosphorylation:

T4 Polynucleotide Kinase:

#EK0032; Fermentas Life Science; Ordering Partner – Fisher Scientific Austria GmbH, Vienna, Austria.

Adenosine triphosphate (ATP):

#R0441; Thermo Scientific; Ordering Partner – Fisher Scientific Austria GmbH, Vienna, Austria.

2.2.3 DNA amplification:

AluI:

#ER0012; Thermo Scientific; Ordering Partner – Fisher Scientific Austria GmbH, Vienna, Austria.

Ampligase® DNA ligase Kit:

#A30201; Epicentre distributor – Biozym Biotech Trading GmbH, Vienna, Austria.

Bovine Serum Albumin (BSA):

#B900S; New England BioLabs distributor – 65926 Frankfurt am Main, Germany.

Deoxynucleoside triphosphate:

#R0192; Thermo Scientific; Ordering Partner – Fisher Scientific Austria GmbH, Vienna, Austria.

phi29 DNA-polymerase:

#EP0092; Thermo Scientific; Ordering Partner – Fisher Scientific Austria GmbH, Vienna, Austria.

T4-DNA ligase:

#EL0011; Thermo Scientific; Ordering Partner – Fisher Scientific Austria GmbH, Vienna, Austria.

2.2.4 Gel electrophoresis:

6x MassRuler DNA Loading Dye:

#R0621; Thermo Scientific, Ordering Partner – Fisher Scientific Austria GmbH, Vienna, Austria.

GeneRuler 100 bp Plus DNA Ladder 100 to 3000 bp:

#SM0321; Thermo Scientific; Ordering Partner – Fisher Scientific Austria GmbH, Vienna, Austria.

peqGOLD Universal-Agarose:

#35-1020; PEQLAB, 91052 Erlangen, Germany.

SYBR[®] Safe DNA Gel Stain:

#S33102; Life Technology, Vienna, Austria.

Tris(hydroxymethyl)-aminoethane) – Boratic acid – Ethylenediaminetetraacetic acid or TBE-buffer:

#T4415-4L; Sigma-Aldrich, Vienna, Austria.

2.2.5 Programs:

ChemSketch and Inkscape:

These two programs were used to draw the various pictures, such as molecular structures of antibiotics, ECM, etc. They are available for free at:

http://www.chip.de/downloads/ChemSketch_36574377.html

http://www.chip.de/downloads/Inkscape_15274752.html

LabView:

Monitoring program for the LCR meter written by Thomas Maier.

MATLAB R2010b and Microsoft OfficeTM Tools:

These programs were used for simulation, plotting, drawing, etc.

2.2.6 Important parameters & informations:

2.2.6.1 LCR meter:

A sinusoidal voltage with an amplitude of 10 mV was used for all experiments, so that no electrochemical process could take place.

2.2.6.1.1 Frequency range:

For all measurements the frequency range was set from 100 Hz to 1 MHz, but in the case of the test solutions (consisting of differently concentrated KCl solutions) 50 frequency data

points were applied at each experiment, whereas in isothermal amplification only 20 different frequencies were carried out. This decrease of data points was done in order to increase the speed of analysis.

2.2.6.1.2 Weakness of LCR meter:

Below 100 Hz the measured data vary enormously, which is the reason why they were not measured. The reason for this tremendous variation is shown in the calculation below:

$$R = \frac{U}{I} \quad \rightarrow \quad I = \frac{U}{R} \quad \rightarrow \quad I = \frac{10^{-2}}{10^8} = 10^{-10} = 100 \text{ pA}$$

Because of the low sinusoidal voltage (10 mV) and high resistance values, especially at lower frequencies, ($\sim 10^8$ Ohm) a very low current flow, ~ 100 picoampere (pA), arises from this fact, which is difficult to resolve. But an increase of the voltage, which would lead to higher currents and also to a better and stable measurement, might also lead to electrochemical processes, so that this solution was not tested.

Around 100 kHz a spontaneous decrease and at 1 MHz an increase of the impedance are visible in nearly all experiments. These two systematic bugs are the more pronounced the higher the resistance or lower the conductivity of the medium is. To overcome these problems two different approaches have been tried. First, to overcome the decrease by ~ 100 kHz the frequency value was changed and second, to solve the increase at 1 MHz the frequency scan was stopped at 960 kHz.

Two other approaches which maybe can lower these phenomena, especially the decrease at 100 kHz, are: first, if this change is induced by the outside, the use of a faraday cage and second, a repeated measuring of a sample to build the average over all measurements. These two solutions have not been tried. One reason for this was that for multiple measurements the probe has to be stable over a certain period of time which is not the case by an isothermal amplification process.

2.2.6.1.3 Open-Short-correction:

Before an experiment was carried out, an Open-Short-correction has to be performed (the position of the switches can be seen in figure 22) in order to eliminate parallel parasitic capacitances from the cables and the LCR meter.

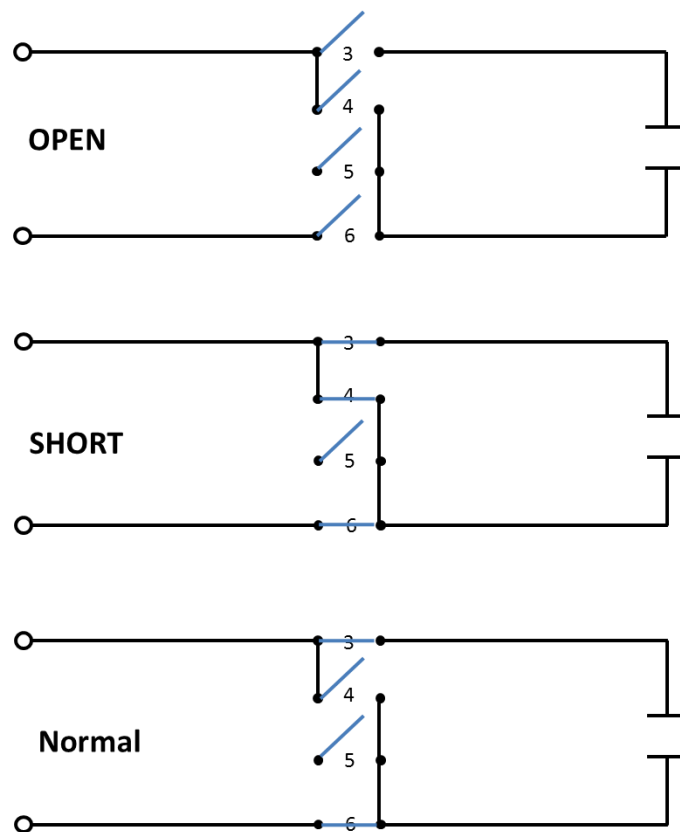


Figure 22: Position of the switches by an Open-Short-correction and a “normal” or ordinary measurement. Before every experiment an Open-Short-correction has to be done to eliminate parasitic capacitances from the cables and the LCR meter.

2.2.6.2 Cleaning procedure - Biosensor RCA bla AIT:

After each experiment the sensor was cleaned according to a strict protocol. First, the 2 ml or 0.2 ml Eppendorf tube, which acts as a reaction chamber, has to be removed, then the system, especially the electrodes has to get rid of liquid under the use of compressed air. Afterwards the electrodes have to be cleaned through immersing them into a new appropriate reaction tube, filled with dH₂O. With compressed air the electrodes has to be dried by removing the liquid. This washing and drying step has to be repeated several times.

2.2.6.3 Gel electrophoresis:

For the separation and analysis of amplified products gel electrophoresis was the method of choice, in which DNA, especially DNA fragments, are separated from each other through an outer electrical field, based on their size. The gel is a cross-linked polymer, made of 2 % agarose. Larger DNA fragments can be separated by lower agarose concentrations and vice versa.

First 150 ml 1x concentrated TBE-buffer and 3 g agarose are mixed together and heated up in a microwave until the agarose is fully dissolved. After a cooling period of 5 minutes 6 µl SYBR[®] Safe DNA gel stain are added and mixed for 5 minutes. Then this mixture is filled into a gel chamber until it gets solid.

The solid gel is given into an electrophoresis chamber: the gel pockets are filled with 8 µl of DNA samples, while the left pocket is filled with 8 µl of GeneRuler 100 bp Plus DNA Ladder to determine the length of the DNA fragments.

After this the electrophoresis was carried out at a constant voltage of 160 V for 50 minutes, and visualized using an UV-Imaging system which made the DNA fragments light up.

2.2.6.4 Biological system:

The whole biological system, the padlock probes, the synthetic DNA, etc. is based on the work of Ivan Barišić (AIT), especially on his dissertation “Characterization and detection of β -lactamases” written in the year 2013. In this document there are all DNA sequences and also further informations available.

2.3 Rolling Circle Amplification:

Before RCA could be carried out, the specific padlock probes have to be combined. Because of this, the four different padlock mixes were made for the 33 clinical relevant β -lactamases, see table 2.

- Padlock Mix 1 (Carbapenemases):

IMI-1, KPC-1, SME-1, IMP-1, IMP-24, VIM-1, VIM-2, NDM-1, OXA-23, OXA-24, OXA-24, OXA-48, OXA-51, OXA-58.

- Padlock Mix 2 (ESBLs):

CTX-M1, CTX-M2, CTX-M8, CTX-M9, CTX-M25, PER-1, RTG-4, SFO-1, VEB-1.

- Padlock Mix 3 (AmpCs):

ACT-1, CMY-1, CMY-2, DHA-1, FOX-1, MIR-1.

- Padlock Mix 4 (NSBLs):

SHV-1, TEM-1, OXA-1, OXA-2.

After the correct combination of the padlock probes, they have to be phosphorylated, so that the DNA ligase has a starting point for the ligation process. The various chemicals (see table 4) were mixed together, put in a thermo cycler at 37 °C for 30 minutes and then heated up to 65 °C for 20 minutes to inactivate the DNA kinase. The thereby obtained padlock mixes, but also the ligated probes from the next step were stored until the moment of use at -20 °C.

Table 4: Phosphorylation protocol of the padlock probes.

	Conc. Stock	Final-MM-Conc.	[50 μ l]
dH₂O			14.00
10x T4 Polynucleotide Kinase Buffer			5.00
ATP [mM]	10.00	1.00	5.00
Padlock Mix 1-4 [nM]	200	100	25.00
T4 Polynucleotide Kinase	10000 U/ml	10 U/50 μ L	1.00

Temperature program:

37 °C	30 minutes
65 °C	20 minutes
-20 °C	forever

Before RCA reaction could take place, the padlock probes have to be ligated. In case of positive amplification reaction synthetic target-DNA, which perfectly fit together with the padlock probe, has to be taken and by a negative control deionized water was used instead of DNA. This ligation step was done at a thermo cycler as it is necessary to heat up the reaction mixture to 95 °C to activate DNA ligase, which may destroy or damage the passivation layer of the electrodes.

Table 5: RCA protocol. Step 1: Hybridization and Ligation of the padlock probes; Step 2: 1st RCA cycle, which was carried out on the Biosensor_RCA_bla_AIT; Step 3: 20 µl of the 1st RCA product were taken and digested; Step 4: 2nd RCA cycle, which was carried out to increase the DNA concentration. Synthetic target-DNA (syn. DNA): 15 µl of each target position - Stock concentration 50 nM - has to be pipetted into the 200 µl Eppendorf micro tube (e.g.: 15 µl of each TEM-1 position - POS.46, 457 and 631). MM is a synonym for Mastermix.

Hybridization and Ligation	Step 1		
	Conc. Stock	Final-MM-Conc.	[90 µl]
syn. DNA [nM]		8.33	45.00
dH₂O			13.50
Padlock Mix # 1 - 4 [nM]	1.00	0.10	9.00
BSA [µg/µl]	2.00	0.20	9.00
10x Ampligase Buffer			9.00
Ampligase [U/µl]	5.00	0.25	4.50

Temperature program:

95 °C	5 minutes
60 °C	60 minutes
95 °C	2 minutes
-20 °C	forever

1st RCA	Step 2		
	Conc. Stock	Final-MM-Conc.	[180 µl]
Step 1 product			90.00
dH₂O			40.50
dNTP [mM]	2.50	0.125	9.00
10x phi29 Buffer			18.00
phi29 DNA-polymerase [U/µl]	10.00	0.20	3.60
Oligo 2 C2CA [nM]	50.00	0.25	0.90
BSA [µg/µl]	2.00	0.20	18.00

Temperature program:

37 °C	40 minutes
65 °C	2 minutes
4 °C	forever

Digestion	Step 3		
	Conc. Stock	Final-MM-Conc.	[25 µl]
Step 2 product			20.00
dH₂O			3.42
BSA [µg/µl]	2.00	0.20	0.50
10x phi29 Buffer			0.50
AluI [U/µl]	10.00	1.00	0.50
Oligo 1 C2CA [µM]	50.00	0.80	0.08

Temperature program:

37 °C	5 minutes
65 °C	5 minutes
4 °C	forever

Ligation and 2nd RCA	Step 4		
	Conc. Stock	Final-MM-Conc.	[35 µl]
Step 3 product			25.00
dH₂O			3.20
BSA [µg/µl]	2.00	0.20	1.00
10x phi29 Buffer			1.00
T4 DNA Ligase [U/µl]	1.00	0.05	0.50
ATP [mM]	10.00	3.33	3.00
dNTP [mM]	2.50	0.25	1.00
phi29 DNA-polymerase [U/µl]	10.00	0.33	0.30

Temperature program:

37 °C	40 minutes
65 °C	2 minutes
4 °C	forever

After the hybridization and ligation step (step 1 of the RCA protocol, see table 5) the isothermal amplification reaction (step 2) was carried out on Biosensor_RCA_bla_AIT. For this purpose the cleaned sensor with a new 200 µl Eppendorf micro tube, also called as reaction tube, was fixed at the thermo mixer at 37 °C. Before the 1st RCA cycle was conducted an Open-Short-correction has to be done to eliminate parasitic capacitances.

After 40 minutes the phi29 DNA-polymerase was inactivated by heating the reaction mixture up to 65 °C for 2 minutes, the sample was taken out of the reaction tube and the sensor has to be cleaned.

From this 1st RCA product 20 µl were taken and digested, as described in step 3.

Thereafter, the 2nd RCA cycle (step 4) was achieved to increase the DNA concentration for gel electrophoresis. Afterwards, in order to cut the thereby obtained long ss-DNA strand into shorter DNA fragments, the digestion step has to be repeated.

Finally, a mixture of 3 µl long ss-DNA and 3 µl of short ss-DNA fragments were mixed together with 2 µl of a DNA-Loading dye and were analyzed via gel electrophoresis.

After 50 minutes runtime the gel was visualized under UV light that caused the DNA fragments to light up.

3 Results & Discussion:

3.1 Biosensor_Virus Infineon:

Figure 23 represents an overview over the four different interdigitated electrode (IDEs) geometries, labeled V1, V2, V3 and V4, provided by Infineon, Villach. Table 6 represents the geometrical parameters of the individual fields. V1 has the greatest finger structure and the lowest number of fingers and V4 has the lowest finger structure and the highest number of fingers. The hexagonal structures on the left respectively right side of the chip are the contact pads.

Table 6: Parameters of the four different IDEs structures V1, V2, V3 and V4. The passivation layer consists of silicon nitride and has a thickness of $\sim 4 \mu\text{m}$.

	V1	V2	V3	V4
Length of a finger [μm]	813.0	813.0	813.0	813.0
Distance between two fingers [μm]	4.0	3.0	2.5	2.0
Thickness of one finger [μm]	10.0	6.0	4.2	3.0
Number of fingers	50	74	98	134

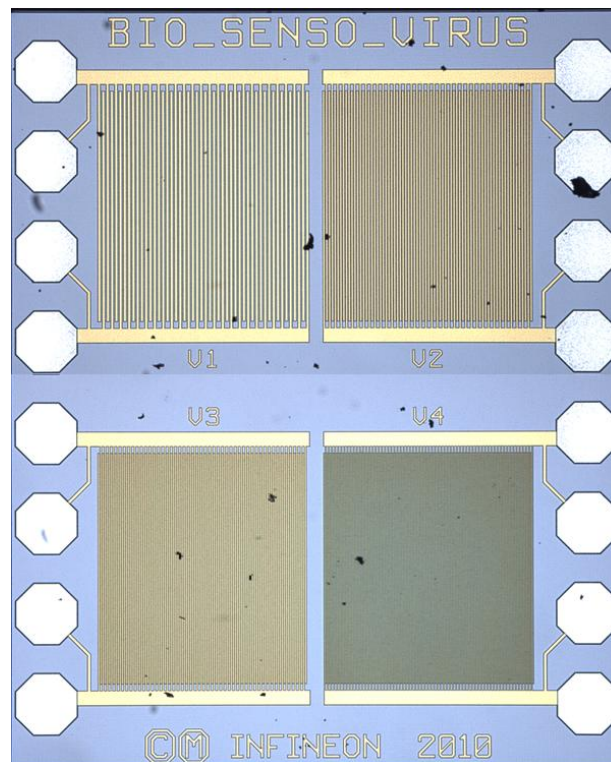


Figure 23: Image of Biosensor_Virus provided by Infineon, Villach. The different IDEs structures, V1 to V4, are visible. For parameters see table 6.

In order to test the suitability of this type of structure for the detection of isothermal amplified DNA some preliminary tests were performed. First the chip was fixed with silver paste on a printed circuit board (PCB) and then the bonding pads were electrically connected to the PCB with gold wires using an ultrasonic wedge bonder. Soldered wires were used to connect the PCB to the LCR meter. By using a microscope a few micro liters of dH₂O were added onto the chip (see figure 24) and a frequency scan was carried out. Afterwards some KCl-crystals were added to the liquid and after a few minutes, when KCl was dissolved, the scan was repeated.

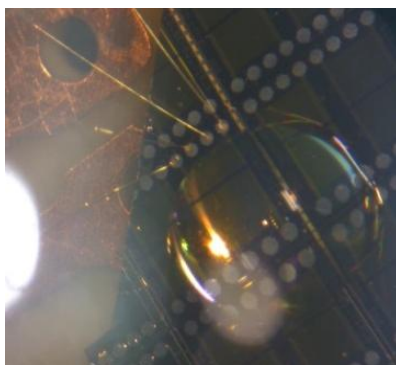


Figure 24: Image of a filled chip, taken through the eyepiece of a microscope. The wires are not in contact with the liquid.

The results of these basic experiments are depicted in figure 25, where ABS-Z is plotted against the frequency. At the high frequency side of the spectrum, the impedance measured for dH₂O (red solid line) shows a slight shoulder, whereas the KCl solution (black solid line) is a straight line. These results are in good qualitative agreement with figure 19, if one assumes that the maximum measurement frequency (1 MHz) corresponds to ν_1 in figure 19. The shoulder in the impedance for dH₂O seems to correspond to the shoulder for R1 in figure 19, the straight line for the KCl solution in figure 25 to that in figure 19 for R2 and R3.

The RCA, however, does not take place in deionized water, but requires a buffer medium with high ionic concentration. The conductivity of this medium will be several orders of magnitude higher, requiring measurement frequencies much higher than 1 MHz. This leads to the conclusion that this type of sensor cannot be used for detection of isothermal amplified DNA with standard experimental equipment.

To fulfill the goal of this thesis, a new sensor for the monitoring of RCA had to be fabricated, which had to meet the following requirements:

1. conductivity measurement of RCA solution
2. the sensor must be operated in a temperature stabilized environment at 37 °C
3. stable operation over duration of amplification reaction (avoid evaporation)

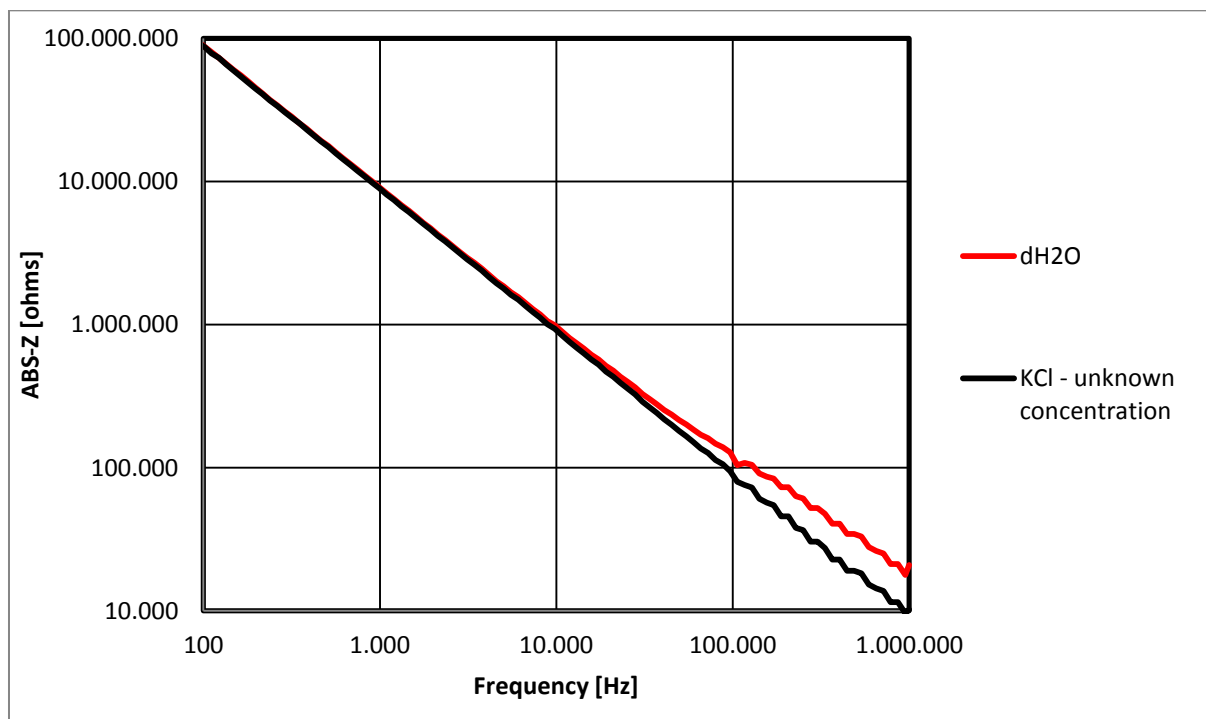


Figure 25: $ABS-Z$ vs. frequency – Biosensor_Virus_Infineon – structure V1. Parameters of the four IDEs are shown in table 6. It can be seen that this biosensor is in the so called $C_{coupled}$ region (corresponds to v_1 on figure 19), which leads to the conclusion that this biosensor is not appropriate for our application.

3.2 Biosensor RCA bla AIT:

3.2.1 Sensor setup and preliminary tests:

Because of the high coupling and low parasitic capacitances a passivated wire, 150 μm thick with a $\sim 6\text{ }\mu\text{m}$ silicon nitride passivation layer, which acts as an electrode, were used for the sensor setup.

To determine the functionality of a sensor (range of the conductivity measurements) it is first tested with differently concentrated potassium chloride solutions (100 μM , 1 mM, 10 mM, 100 mM and 1 M) and also phi29 buffer, which represents the basic buffer system during RCA reaction.

Bearing in mind that the phi29 buffer, in the correct dilution (1x), is a highly concentrated solution, consisting of 50 mM Tris-HCl, 10 mM magnesium chloride (MgCl_2), 10 mM ammonium sulfate ($(\text{NH}_4)_2\text{SO}_4$) and 4 mM dithiothreitol (DTT), which is best comparable with 100 mM KCl.

An Adaption of geometrical parameters by the use of a glass separator or the montage of capillaries was done in order to make the sensor fit for online isothermal amplification reaction.

3.2.1.1 Electrodes with and without a glass separator in between:

Figure 26 represents two images of a 2 ml based sensor where the wires were formed to loops and separated from each other by a plastic spacer. The wires, cables and coding switch were soldered on a perforated plate that acts as a basic framework.

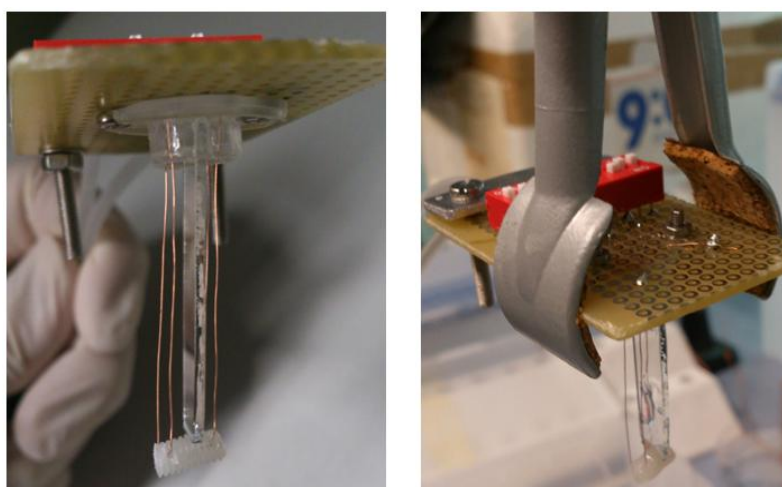


Figure 26: Two images of the 2 ml sensor. The electrodes are separated from each other by a plastic spacer, moreover a removable glass slide is fixed in between the electrodes to increase the resistance of the liquid.

After the fabrication of this system the impedance spectra of 1.8 ml of dH₂O and differently concentrated KCl solutions were measured. The results of these measurements are shown in figure 27 (solid lines). It can be seen that this sensor is able to measure a difference in conductivities between dH₂O and 1 mM KCl. In comparison to the results of the biosensor provided by Infineon, this constitutes a great progress. However, the RCA reaction buffer (phi29 buffer) is much more concentrated, best comparable with 100 mM KCl solution, because they have similar salt concentrations. To further increase the resistance a glass slide, ~3 mm thickness, was placed between the electrodes to separate them from each other (see figure 26). When you compare the results from no glass separator with the curves where a glass slide is fixed between the electrodes it can be seen that using a glass separator (dashed lines) improves the results only slightly.

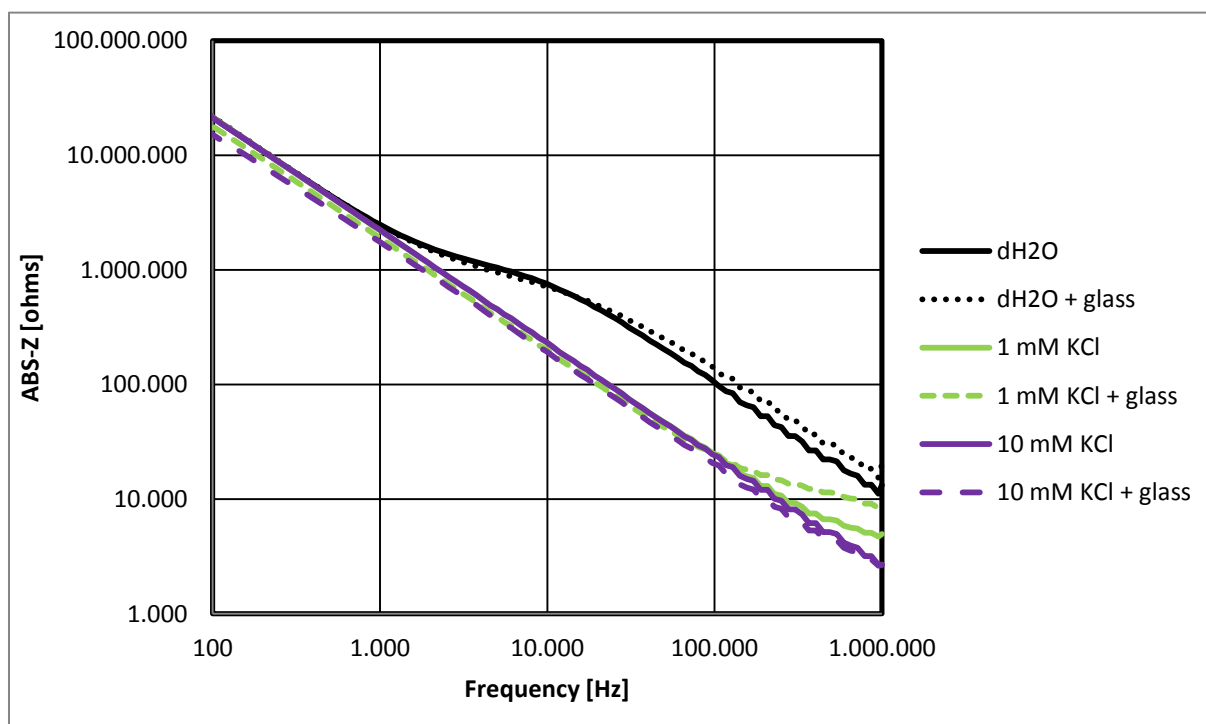


Figure 27: ABS-Z vs. frequency of differently concentrated KCl solutions in a 2 ml reaction tube. The wires are separated from each other in one case by a glass slide in between them, represented by the addition "+ glass". In the other case the separator was removed. With a glass separator an earlier appearance of the plateau is observable.

But all in all, these first results show that the choice of the wires as electrodes was quite good, because:

- the wires have a good and stable passivation layer
- coupling capacity looks promising

So the next step would be to increase the resistance of the liquid and so shift the range of conductivity measurements in measureable frequency region.

3.2.1.2 Electrodes surrounded by glass capillaries:

To further shift the measurement range of the sensor to higher conductivities, the electrodes were surrounded by glass capillaries to increase the resistance again. A smaller Eppendorf micro tube with a total volume of 200 μl was used to minimize consumption of reagents.

Figure 28 represents the final sensor setup. It is a self-built system consisting of a perforated plate as the framework where everything else, such as the coding switch for Open-Short-correction, the wires and cables was soldered on. Each wire is surrounded by a glass capillary, $\sim 300\text{ }\mu\text{m}$ thickness, to increase the resistance of the liquid again.

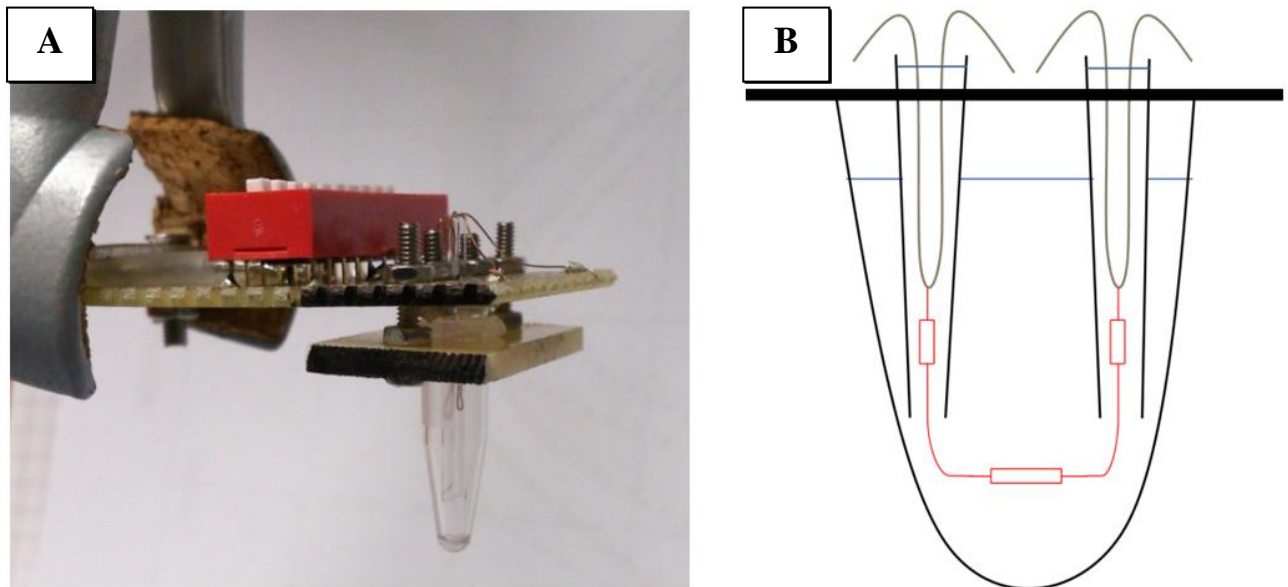


Figure 28: (A) Image and (B) schematic overview of the final sensor, called Biosensor_RCA_bla_AIT. Through capillary force the liquid is pumped up, illustrated by the blue lines. In the case of positive DNA amplification the resistance of the medium would change and this can be measured.

As before, this new 0.2 ml sensor was also initially tested with 180 μ l of differently concentrated KCl solutions to determine its suitability for online isothermal amplification. The results of these various tests are represented in figures 29 to 31.

Figure 29 represents the results of ABS-Z plotted against frequency. Between 100 μ M and 100 mM concentrated KCl solutions the different plateaus are observable. With increasing salt concentration this plateau is shifted to higher frequencies. At 100 mM and phi29 buffer the beginning of the plateaus are visible. The shoulder of dH₂O and 1 M KCl are no longer detectable, which displays the detection limit of this sensor.

Furthermore the difference at impedance between phi29 buffer and 100 mM KCl, which have similar conductivities, is increasing with higher frequencies. This leads to the conclusion that the differences of conductivity of phi29 buffer might be better at higher frequencies.

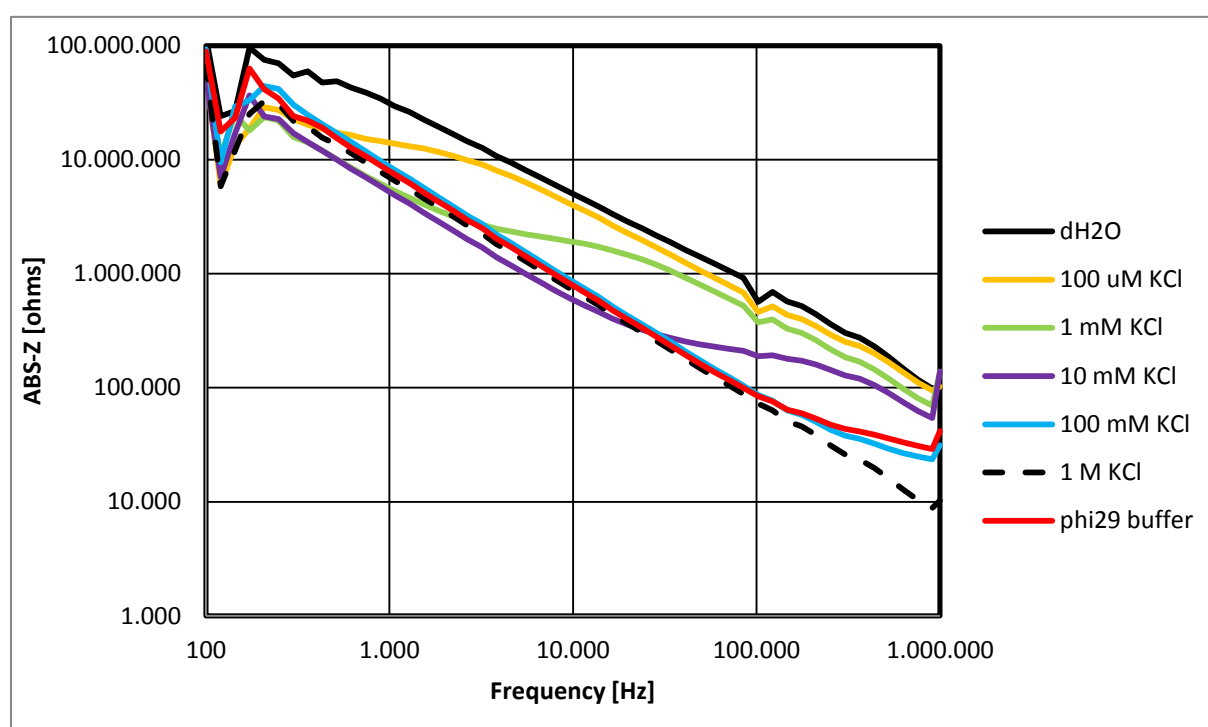


Figure 29: ABS-Z vs. frequency – Biosensor_RCA_bla_AIT – of differently concentrated KCl solutions. With higher salt concentrations the characteristic change in impedance is shifted to higher frequencies.

The real part of impedance is shown in figure 30. Higher salt concentrations lead to lower values of the real part and a bending of the curve at higher frequencies, which is in good accordance with the simulations (figure 20). At low frequencies, however, the measured values deviate from the expected flat distribution.

These deviations, which become more pronounced in high salt concentrations, show the limitations of the LCR meter. At low frequencies, the imaginary part is several magnitudes higher than the real part, which cannot be detected by the LCR meter.

Because of these limitations ABS-Z or phase is therefore used to characterize the conductivity.

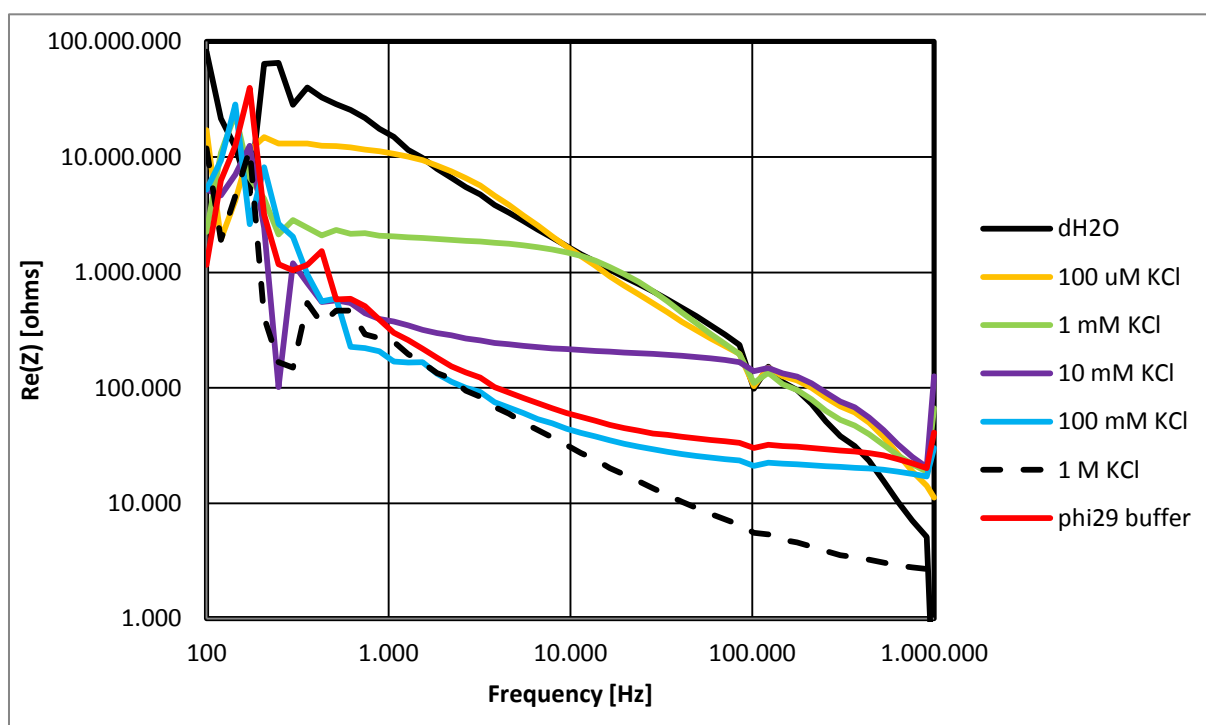


Figure 30: Re(Z) vs. frequency – Biosensor_RCA_bla_AIT – of differently concentrated KCl solutions. Here the limitations of the LCR meter can be seen: At low frequencies, the imaginary part is several magnitudes higher than the real part, especially at high salt concentrations, which cannot be detected by the LCR meter.

Figure 31 represents the data of phase, converted into degree by dividing the result by π and then multiplying it with 180, plotted against frequency. The positions of the observed peaks correspond to the shoulders in ABS-Z (figure 29). An increase of the salt concentration leads to a shift of the curve maximum to higher frequencies. Outside the peaks, the phase approaches -90° , which corresponds to a purely capacitive behavior. At this figure the weaknesses of the LCR meter, described in chapter 2.2.6.1.2, are observable. The two systematic bugs, first at 100 kHz, which decreases with increasing salt concentration, and second at 1 MHz, which is not influenced by the conductivity of the medium.

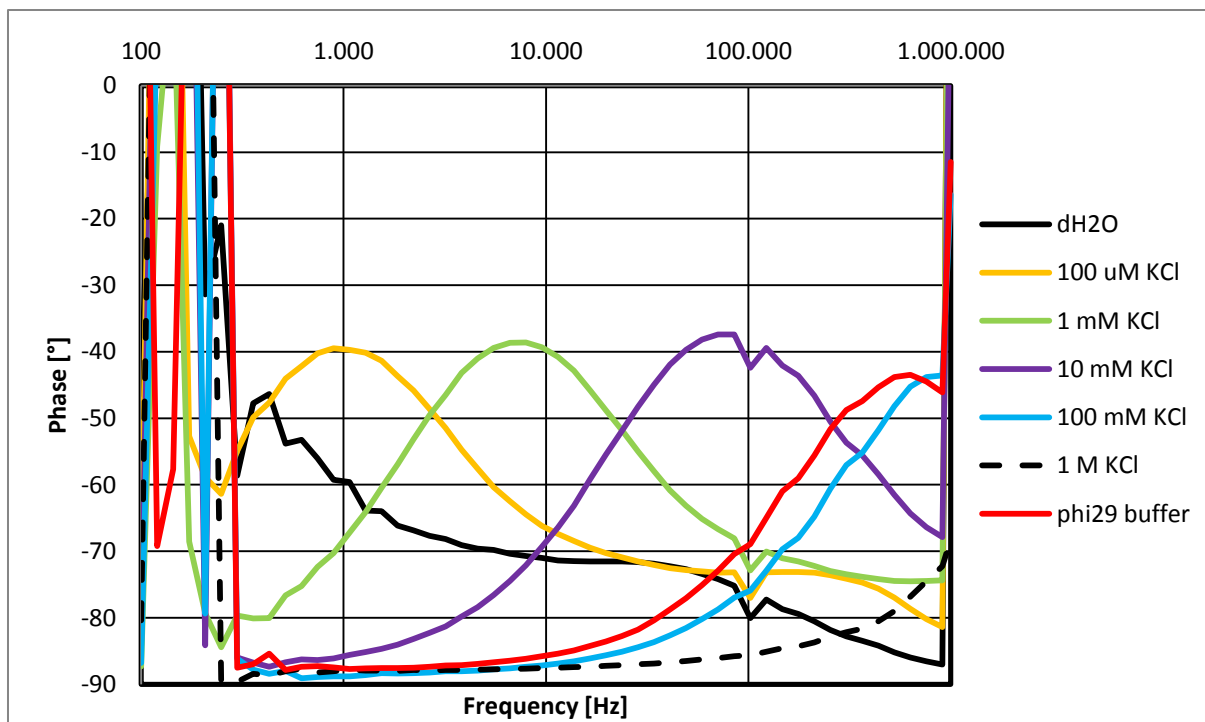


Figure 31: Phase vs. frequency – Biosensor_RCA_bla_AIT – of differently concentrated KCl solutions. With increasing salt concentration the phase maximum is shifted to higher frequencies.

However, only one measurement of each concentration is shown here. Generally, the results show a higher fluctuation at low frequencies as well as a larger standard derivation. With increasing frequencies this phenomenon decreases rapidly. For example, at ~800 kHz the standard derivation of four measurements is about 0.1 % or even less.

All three figures also show that at less than 500 Hz the fluctuations of the signals are very high and this indicates that below 500 Hz or even 1 kHz the data are not useful for analyses. Above all, these results show – with the restrictions mentioned – good agreement with the simulation done in chapter 1.4.5 and that the sensor now operates in the correct frequency range, which leads to the conclusion that this sensor is suitable for the RCA detection.

3.2.1.3 The Influence of the filling levels and the number of glass layers:

The influence of different filling levels (50, 70, 90, 120, 150 and 180 μ l) was also tested with one and two glass capillaries at each electrode. For these experiments a new sensor was built and 100 mM KCl solution was used since this concentration shows similar results as the phi29 buffer, but is much cheaper. The measurements were carried out under room

temperature so that the sample changing became much easier and the Open-Short-correction had to be done only once at the beginning.

The results of the experiments with one capillary at each electrode are represented in figure 32 and 33. An increasing filling level leads to a shift of phase maximum to lower frequencies combined with a decrease of the maximum, which might be explained by the change of the coupling and parasitic capacitances by a variation of the filling level, see figure 21.

It seems that with increasing filling levels, first both coupling and parasitic capacitances change to higher values until a specific level, somewhere between 70 and 90 μl , and then only the parasitic capacitance increases.

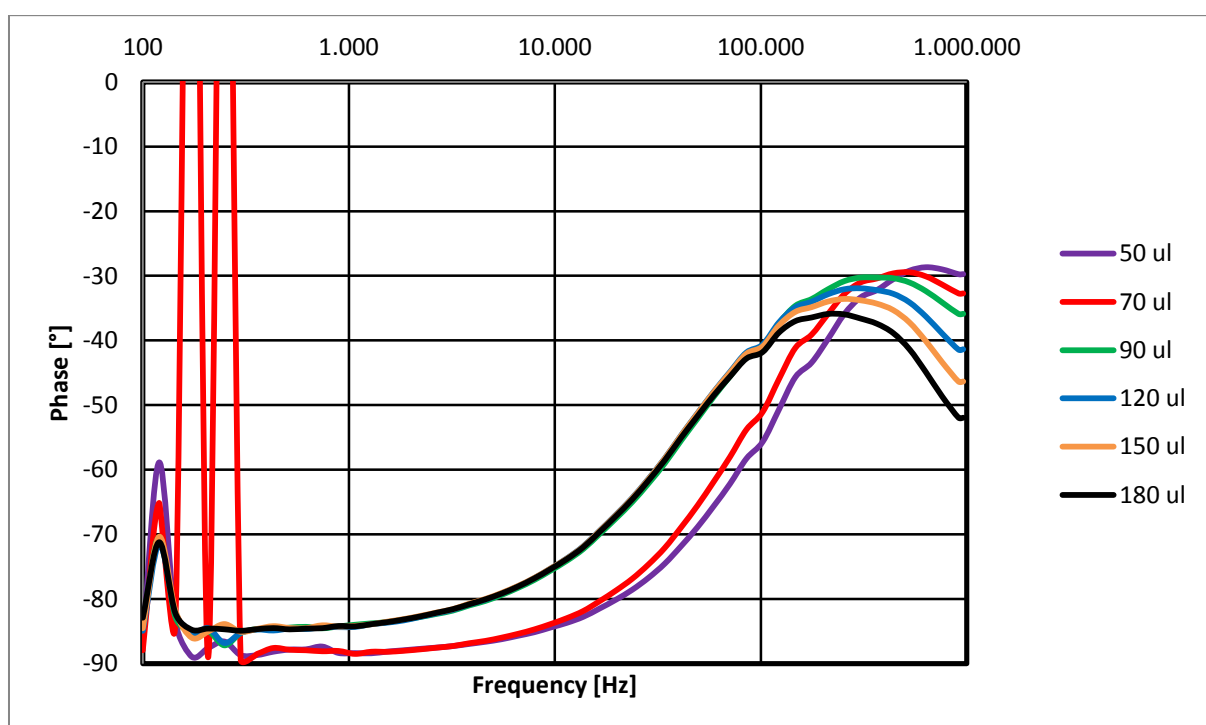


Figure 32: Phase vs. frequency – Biosensor_RCA_bla_AIT – of 100 mM KCl solution at different filling levels; the electrodes are surrounded by one layer of glass (= one capillary at each wire). A higher filling level leads to a shift of the phase maximum to lower frequencies combined with a simultaneous decrease of the maximum.

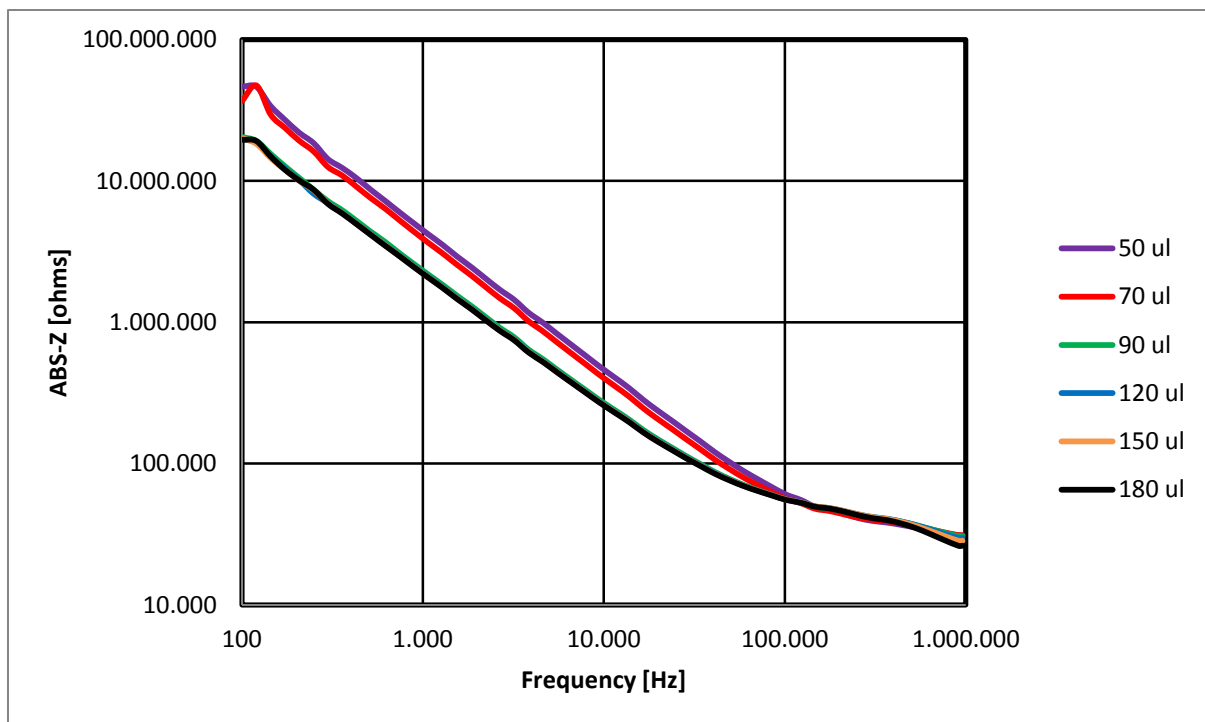


Figure 33: ABS-Z vs. frequency – Biosensor_RCA_bla_AIT – of 100 mM KCl solution at different filling levels; the electrodes are surrounded by one layer of glass (= one capillary at each wire). With increasing filling levels the ABS-Z value at the beginning changes to lower values until a certain level (between 70 and 90 μl).

The double coating of the electrodes (see figure 34 and 35) does not lead to such a tremendous change in phase and ABS-Z as it can be seen in the electrodes with one glass layer. Especially the variation of coupling capacity at lower filling levels is not so great pronounced. In general the results are more stable in comparison to one glass capillary.

As these experiments were done at the end of this master thesis, first the online isothermal amplification measurements were not repeated with two glass layers at each wire and second, further investigations were not done because of time and so this phenomenon is not perfectly understood.

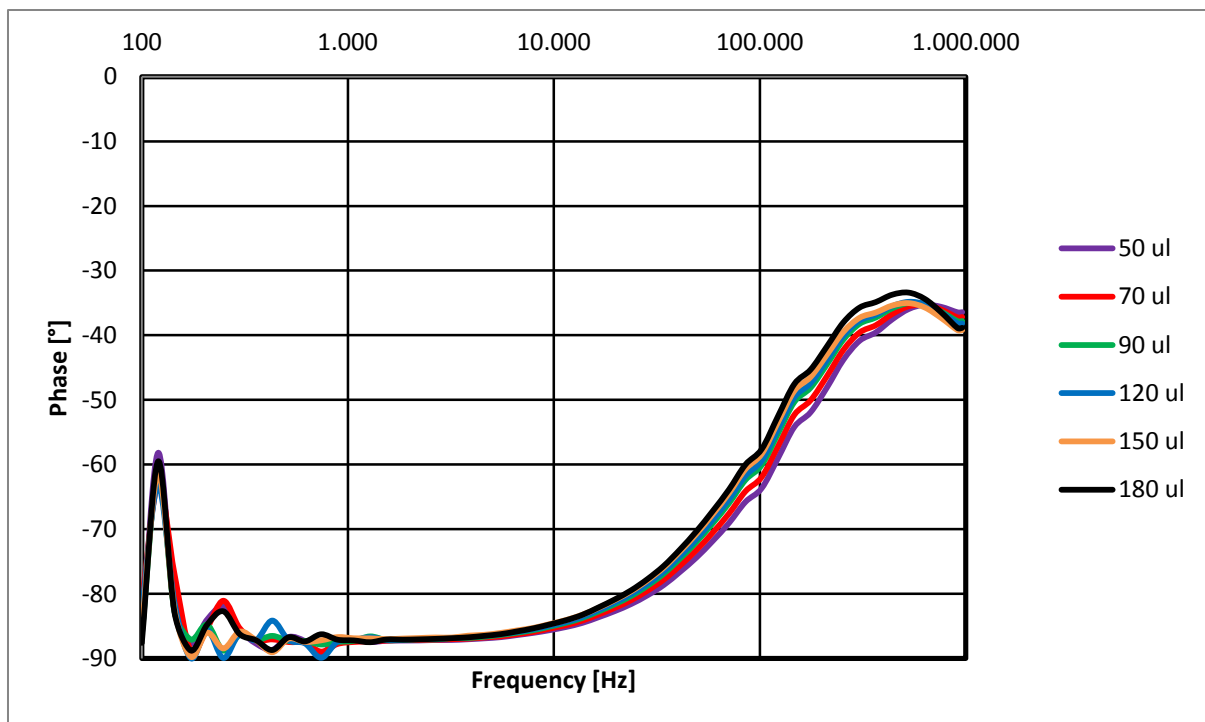


Figure 34: Phase vs. frequency – Biosensor_RCA_bla_AIT – of 100 mM KCl solution at different filling levels; the electrodes are surrounded with two layers of glass (= two capillaries at each wire). A higher filling level does not lead to such a change of the phase maximum.

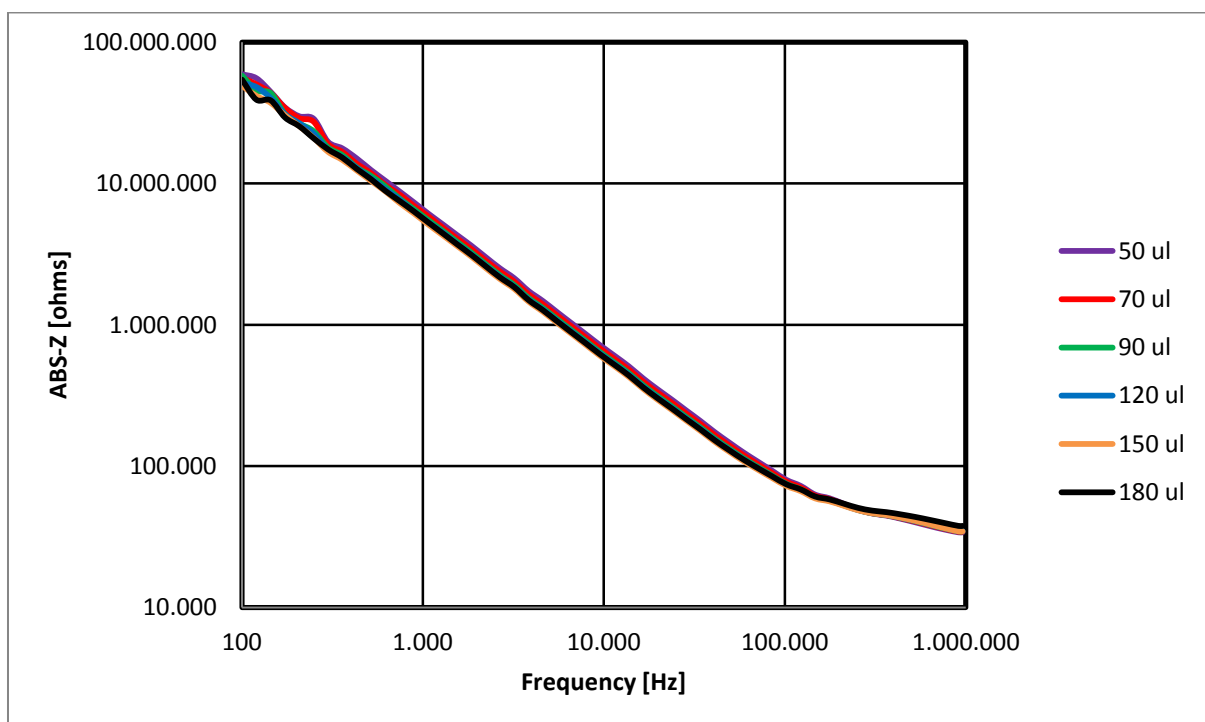


Figure 35: ABS-Z vs. frequency – Biosensor_RCA_bla_AIT – of 100 mM KCl solution at different filling levels; the electrodes are surrounded with two layers of glass (= two capillaries at each wire). With increasing filling level nearly no difference between 50 to 180 µl is observable.

3.2.1.4 The Influence of temperature:

The final sensor was also tested at three different temperatures, first in order to determine the influence of temperature to the resulting signal, especially the initial value of the plateau and second to verify the stability of passivation layer. For these experiments 180 μl of phi29 buffer were filled into the reaction tube and the impedance at room temperature (RT), 37 °C and 65 °C were measured. As can be seen in figure 36 the different temperatures have an influence onto the impedance. With increasing temperature the initial change of the impedance curve is shifted to higher frequencies and lower impedance values. This temperature dependency of impedance was one of the reasons why phi29 DNA-polymerase and not the BST-polymerase was taken for isothermal amplification, because the phi29 DNA-polymerase works at lower temperatures. But also the stability and the capacity to synthesis (~70.000 nt without dissociating from the DNA template) were crucial (Dean *et al.* 2001). However, the displayed results show that the passivation layer was not influenced or even damaged by the higher temperatures, which was the main goal by these experiments.

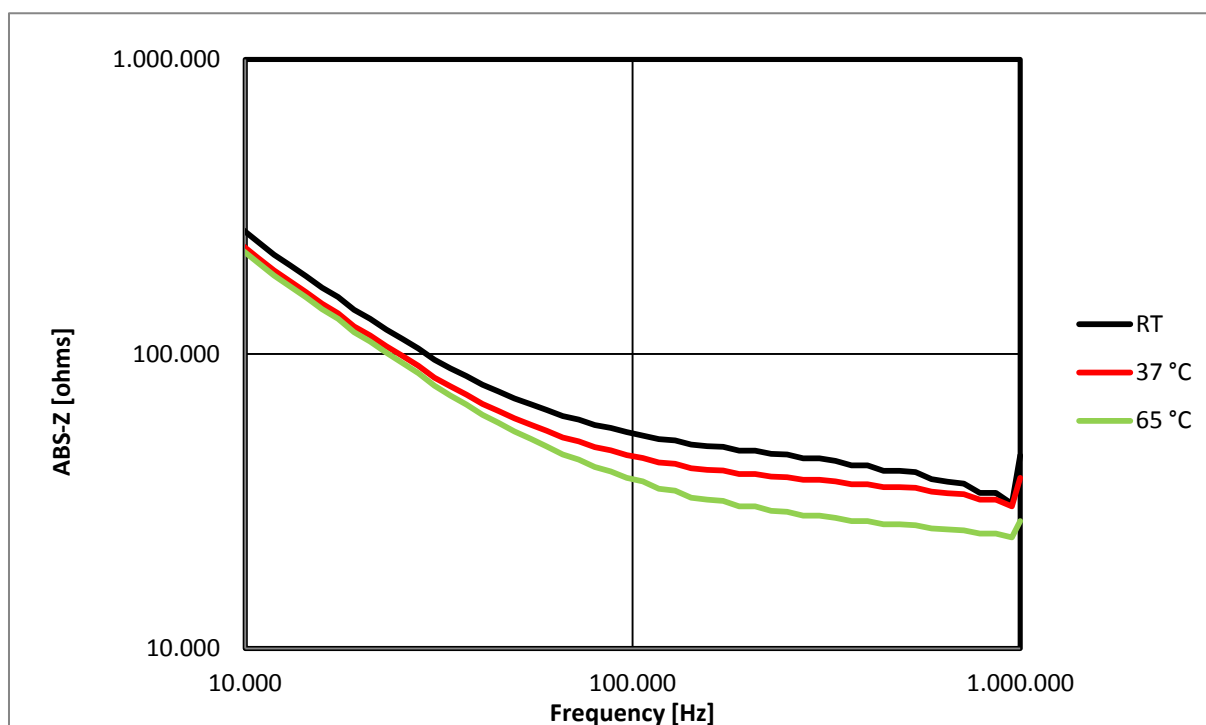


Figure 36: ABS-Z vs. frequency (10 kHz – 1 MHz) of phi29 buffer at different temperatures (RT, 37 °C and 65 °C). A temperature increase leads to a shift to lower impedance values.

3.2.2 Isothermal amplification:

After these preliminary tests, the sensor was used to monitor an isothermal amplification reaction. For that a new reaction tube with 180 μ l of the RCA reaction mix for the 1st RCA cycle without the phi29 DNA-polymerase is fixed onto the system. Then the sensor with the filled tube is mounted at the thermo mixer at 37 °C. After 15 minutes the phi29 DNA-polymerase is pipetted into the reaction mixture and the frequency scan from 100 Hz to 960 kHz (20 different frequencies) began. In comparison to positive amplification products where synthetic target-DNA is used in the ligation step (see table 5 – step 1) deionized water is used by negative controls.

Figure 37 and 38 represent the data, ABS-Z plotted against frequency, of a positive and a negative control, respectively. Figure 37 shows that the impedance shifts to higher values with progressive reaction duration, whereas no such shift is visible in figure 38. The impedance shift increases with growing frequencies.

The impedance spectra taken at 1200 sec and 2100 sec are practically identical, indicating that the amplification reaction is finished after 1200 sec, which may indicate a depletion of the phi29 DNA-polymerase or some other causes, such as the absence of dNTPs.

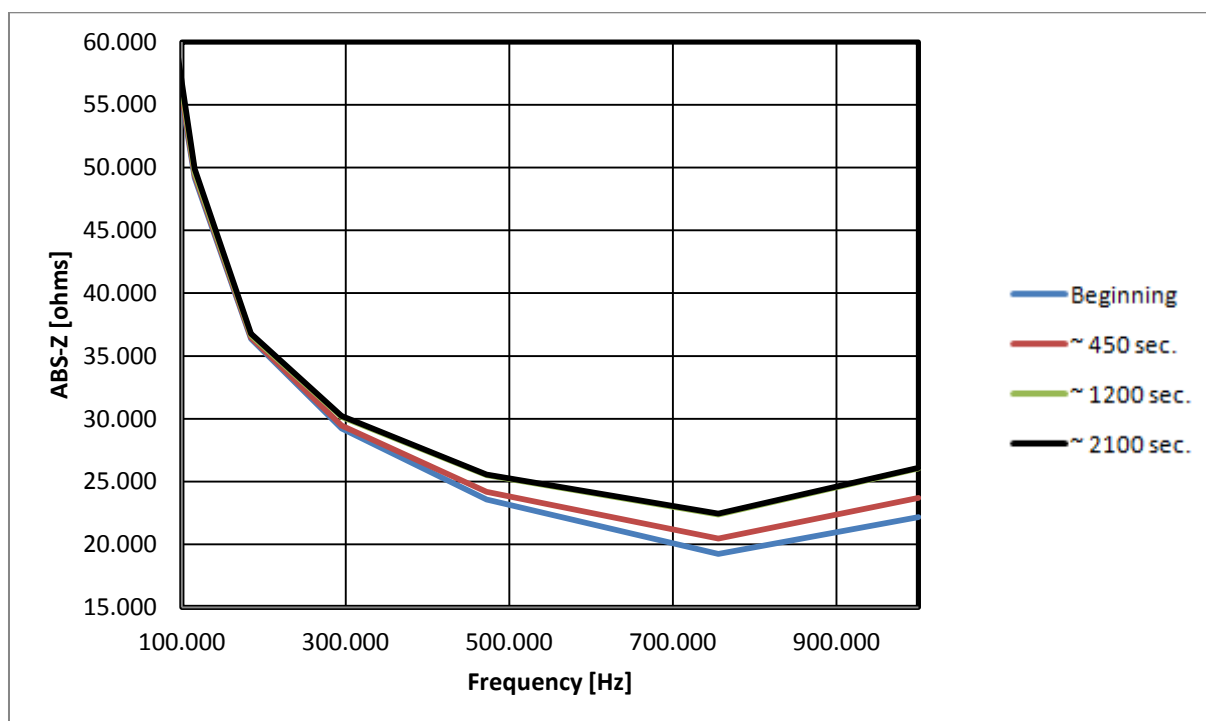


Figure 37: ABS-Z vs. frequency (100 kHz – 960 kHz) of a positive control. A change of the impedance over time is visible. With increasing frequencies this effect is more pronounced.

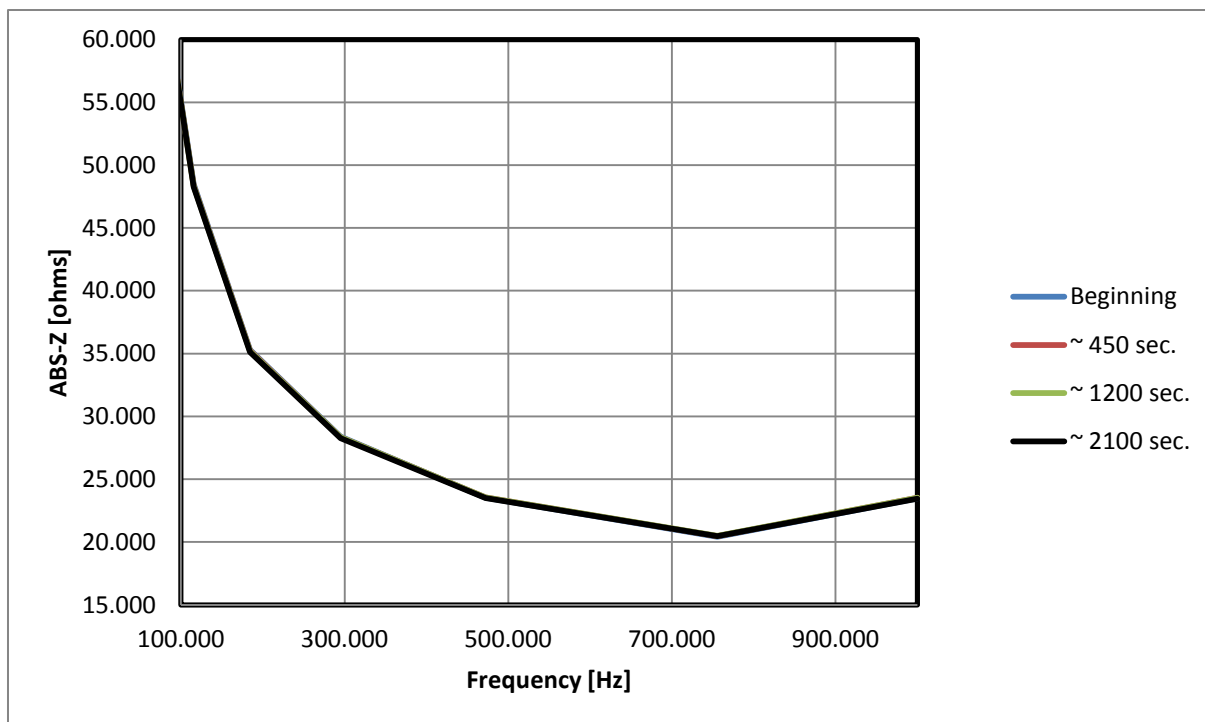


Figure 38: ABS-Z vs. frequency (100 kHz – 960 kHz) of a negative control. No change can be observed.

Figure 39 and 40 show a more detailed time dependence of both three positive and negative amplification reactions at two different frequencies, 184 kHz and 472 kHz.

At 184 kHz the variation of impedance between positive and negative amplification is not distinct, whereas at 472 kHz the increase of the impedance is clearly visible.

Pourmand *et al.* (2006) describes the mechanism of DNA-polymerization in which the result of DNA amplification is an increase in conductivity by the release of a hydrogen proton from the 3'-OH group of a new synthesized DNA strand, which leads to a decrease of impedance. This is the opposite direction of the obtained results, which can be explained by the fact that they only observed the release of a hydrogen proton, inter alia, if the DNA molecule was immobilized on the surface of the electrodes, which was not the case during RCA reaction by our system.

This increase of resistance at a positive amplification is also described in Jiang *et al.* (2012) for a different isothermal amplification method, called LAMP. In their paper they described how they imagine the processes of DNA amplification and their effect on the conductivity. The amplified LAMP product has a negatively charge and by combination of positive ions and positively charged dyes an increase of the resistance of the medium occurs, which they can detect under the use of their special electrodes.

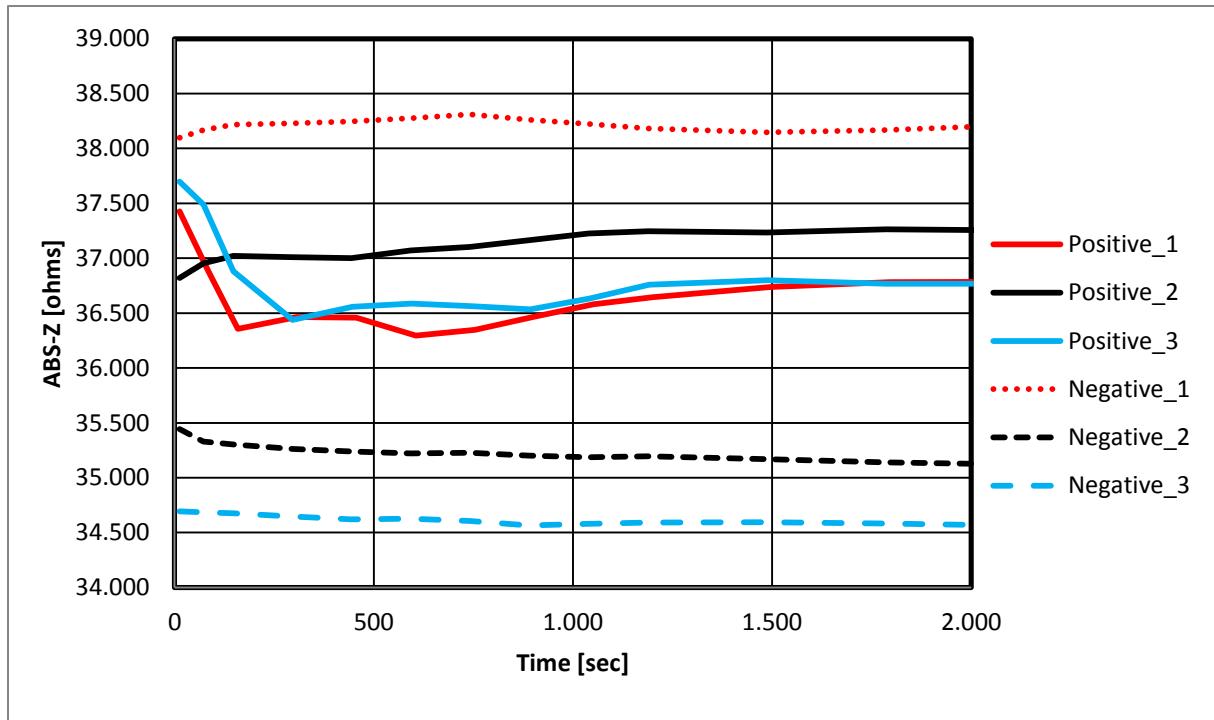


Figure 39: Time dependence of ABS-Z of both three positive (Positive_1-3) and negative (Negative_1-3) controls at 184 kHz. At this frequency no clear differences between positive and negative controls are visible.

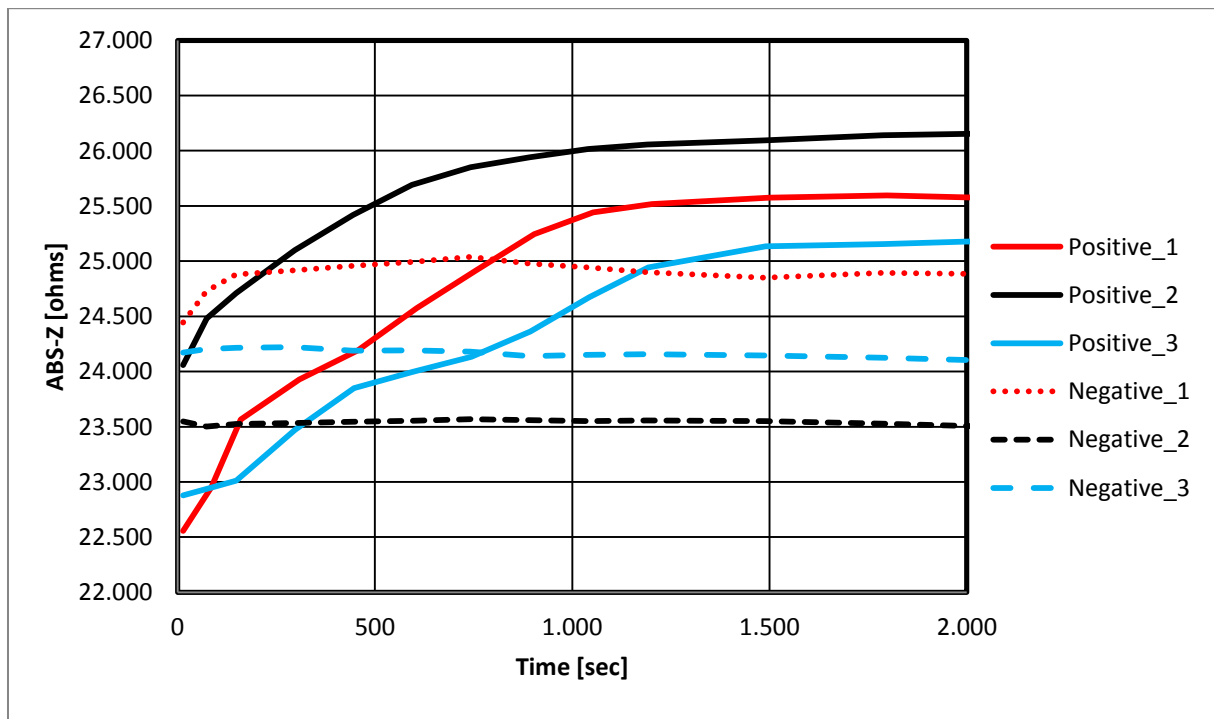


Figure 40: Time dependence of ABS-Z of both three positive (Positive_1-3) and negative (Negative_1-3) controls at 472 kHz. At this frequency a difference between all positive and negative controls is detectable. It is possible to see that with progressing time the impedance of all positive controls increases until around 1200-1500 seconds where it reaches its maximum and becomes a linear behavior.

Nevertheless, DNA amplification is a highly complex biochemical process, during which the concentrations of different ionic species, the size of the DNA molecules and the viscosity of the medium are changed simultaneously, and it is difficult to predict in detail how the conductivity is affected.

Table 7 shows the data of the difference between the beginning and end value of absolute magnitude of impedance (Δ ABS-Z) at three different frequencies (184, 295 and 472 kHz). As can be seen the values – especially the positive amplification – increase with higher frequencies. At 472 kHz the values for the negative controls stay between -142 and 289 ohms, whereas the positive lie between 2056 and 3013 ohms.

Table 7: Results of Δ ABS-Z at 184, 295 and 472 kHz.

Measurement	Frequency [kHz]		
	184	295	472
	Δ ABS-Z [ohms]		
Positive_1	-642	600	3013
Positive_2	406	1180	2056
Positive_3	-844	313	2379
Negative_1	-28	80	289
Negative_2	-372	-274	-83
Negative_3	-172	-232	-142

To control the amplification results gel electrophoresis was chosen. Figure 41 demonstrates such amplification products, where only amplification works at positive controls, and negative controls were not amplified. On the gel three different major DNA fragments can be observed in every positive probe, the first long ss-DNA fragment (few kb) remains at the gel pocket, because it is too long to be separated by a 2 % agarose gel. Followed by the second fragment, which constitutes linear ss-DNA, and the third one, which is the circularized probe. But even so called lubrication bands are observable.

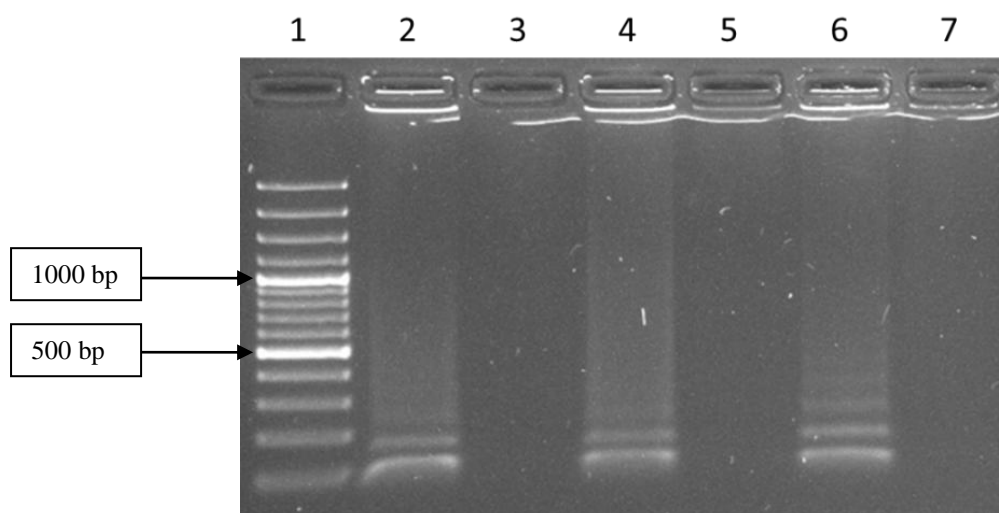


Figure 41: Image of agarose gel electrophoresis. Position 1: GeneRuler 100 bp Plus DNA Ladder; Position 2: Positive_1; Position 3: Negative_1; Position 4: Positive_2; Position 5: Negative_2; Position 6: Positive_3; Position 7: Negative_3. Three major DNA fragments can be detected by positive controls. The first consists the long ss-DNA that remains at the gel pocket because it is too large to get through the pores of the matrix, the second and the third ones are the short ss-DNA fragments after a digestion step, whereas the second represents linear ss-DNA and the shortest fragment the circularized padlock probes.

3.2.2.1 Comparison of different amplification temperatures:

The main motivation behind these measurements was to determine the differences in kinetics between 30 °C and 37 °C amplification temperature.

The experiments with lower amplification temperature, 30 °C, were carried out while only the temperature and nothing else was changed. The comparison of the 30 °C results (figure 42) and the results at 37 °C (figure 40) leads to the conclusion that the results show an inconclusive behavior because on the one hand the positive controls at 30 °C are less pronounced as it is the case at 37 °C and on the other hand the negative controls are not so stable at a lower temperature.

In figure 42 only the data at 472 kHz are represented, at lower frequencies, such as 184 kHz, the curves behave as described in chapter 3.2.2.

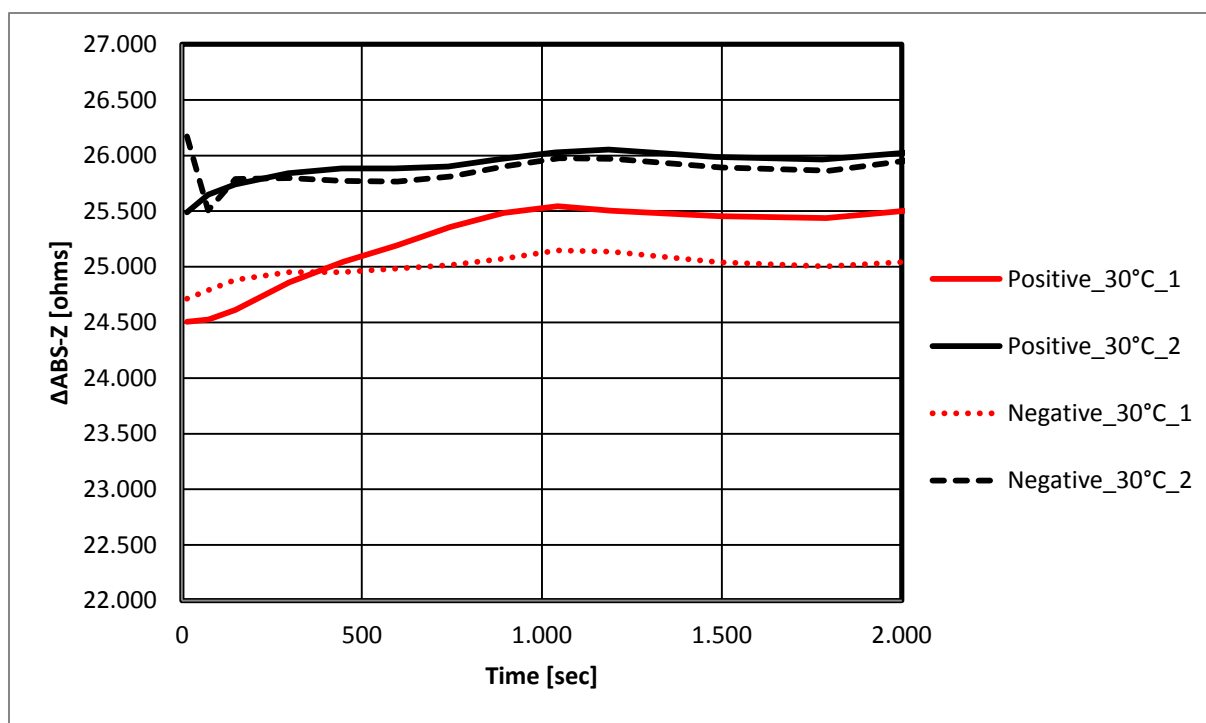


Figure 42: Time dependence of ABS-Z of both two positive (Positive_30°C_1-2) and negative controls (Negative_30°C_1-2) at 472 kHz (30 °C). In comparison to the results at 37 °C amplification temperature (figure 40) there is no such clear difference between positive amplifications and negative controls.

3.2.2.2 The Influence of different target-DNA concentrations:

After confirming that this sensor works for the online detection of isothermal DNA amplification, we investigated the effect of different target-DNA concentrations.

It has been tried to vary the concentration of the synthetic target-DNA both to lower and higher values. The results of these experiments are shown in figure 43, where $\Delta\text{ABS-Z}$ is plotted against the initial target-DNA concentration. At most concentrations several measurements were carried out, where in some cases (0.51 and 4.16 nM target-DNA concentration) only one experiment was conducted in order to save time and money.

An increase of target-DNA leads to an increase of the difference values until a certain concentration. At ~8.32 nM there is a maximum observable and then the values decrease again to higher concentrated target-DNA. A possible explanation for these results might be that the phi29 DNA-polymerase has its optimum concentration in relation to the target-DNA at ~8.32 nM. Normally an increase of the target-DNA concentration would lead to an increase of the signal response, not depending on whether electrochemical or optical methods are used.

But all in all RCA and every other amplification method, such as LAMP or PCR, are highly complex systems, so it is hard to tell in detail what causes this phenomenon without further research.

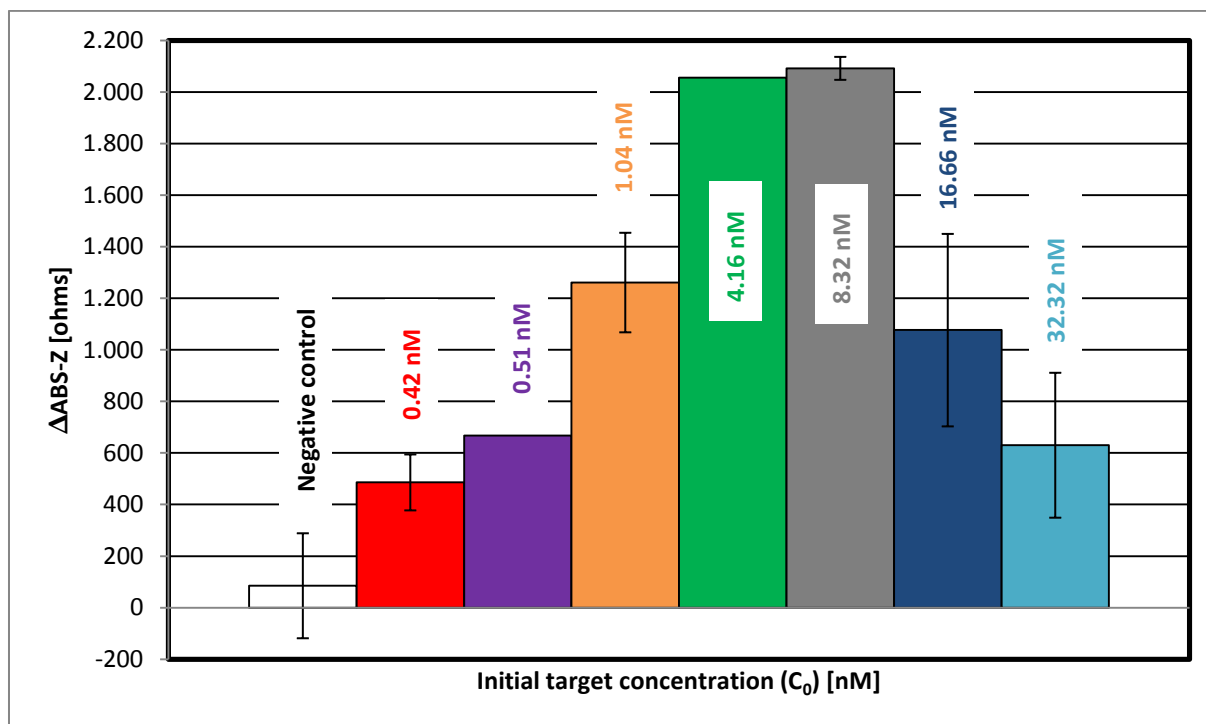


Figure 43: $\Delta\text{ABS-Z}$ at 472 kHz vs. initial target concentration (C_0) calculated on the 1st RCA approach. There is a maximum at ~8.32 nM, hence there is a drop in both directions.

4 Conclusion & Outlook:

During this work two different impedimetric based biosensors, one provided by Infineon and the second, an own developed sensor, were tested for the application of the detection of β -lactam antibiotic resistance genes using Rolling Circle Amplification as the method of choice for DNA amplification.

Unfortunately, the Biosensor_Virus provided by Infineon, Villach, is not a useful tool for the detection of isothermal amplified DNA, as shown in more detail in chapter 3.1, especially if you are limited to 1 MHz, which is the highest frequency value of the used Agilent HP 4248A LCR meter. If you are able to get to higher frequencies, such as GHz, by the use of another LCR meter (which is very cost-intensive), in theory it might be possible to use this kind of chip for the isothermal amplification process. Another possibility is to redesign the chip layout to shift the measurable frequency range to lower frequencies by changing the electrode geometry or the implementation of gaps between the electrodes (Ma *et al.* 2013), but all of these methods would be time- and cost-consuming.

After these basic tests of the Biosensor_Virus and the proof that this IDEs based system does not work for our application, the developing of an own sensor, called Biosensor_RCA_bla_AIT, become the main goal of this thesis. The major motivation behind this development was to get in the measurable frequency range between 20 Hz and 1 MHz.

The results of the different geometrical parameters, first tested with differently concentrated KCl solutions, the development of the biosensor to a working system and different isothermal amplification reactions are all shown in chapter 3.2.

Because of the promising results with differently concentrated KCl solutions isothermal amplification reactions were tested on the sensor. The results are shown in chapter 3.2.2.

With this biosensor we are able to monitor differences between positive and negative controls. In the case of positive amplification reaction impedance is shifted to higher values with progressive reaction duration (figure 37), whereas in the case of negative control no shift is visible (figure 38). The measured DNA amplifications were always confirmed with agarose gel electrophoresis.

Also different target-DNA concentrations (see chapter 3.2.2.2) were tested on this system to determine the influence of the initial target-DNA concentrations onto the Δ ABS-Z values. As you can see in figure 43 there exists a maximum at around 8.32 nM. A possible explanation for these results may be that at this concentration there is an optimal relation between phi29 DNA-polymerase, padlock probes, target-DNA, etc. This leads to the conclusion that in the case of reduced target-DNA a pre-amplification step has to be carried out.

Nevertheless RCA and LAMP, for example, are highly complex biological systems, where the size of the DNA strand, the viscosity of the surrounding medium, for instance, are changed simultaneously, so it is difficult to tell what this phenomenon causes and these results have to be investigated further on.

All in all the obtained results of the Biosensor_RCA_bla_AIT lead to the conclusion that the self-developed sensor is a useful tool for the detection of isothermal amplified DNA, using RCA, and also a possible candidate for further research, especially if you minimize the system to reduce the cost per amplification reaction through change of the geometries to planar electrodes. A possible layout of such a planar sensor is shown in figure 44, where the two passivated electrodes are connected to each other by a microfluidic channel, whereas the material of the microfluidic is the crucial part because some materials can interact or disturb the amplification process described by Kodzius *et al.* 2012. They investigated the inhibitory effect of some microfluidic materials, such as glasses, plastics, silicon oxides, and some other materials on the outcome of the reaction yield by the use of PCR, as amplification method.

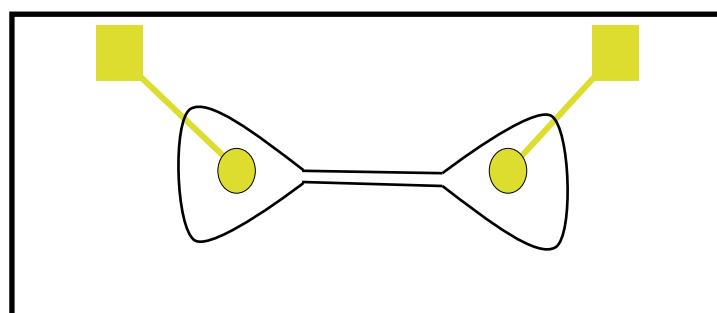


Figure 44: Schematic overview of a sensor based on passivated planar electrodes, which are connected to each other by a microfluidic.

5 References & Appendix:

5.1 List of references:

Aarestrup, F. M.; Seyfarth, A. M.; Emborg, H.-D.; Pedersen, K.; Hendriksen, R. S. and Bager, F. (2001): "Effect of Abolishment of the Use of Antimicrobial Agents for Growth Promotion on Occurrence of Antimicrobial Resistance in Fecal Enterococci from Food Animals in Denmark". In: *Antimicrobial Agents and Chemotherapy* 45 (7), pp. 2054-2059.

Andras, S. C.; Power, J. B.; Cocking, C. E. and Davey, R. M. (2001): "Strategies for Signal Amplification in Nucleic Acid Detection". In: *Molecular Biotechnology* 19, pp. 29-44.

Barišić, I.; Schoenthaler, S.; Ke, R.; Nilsson, M.; Noehammer, C.; Wiesinger-Mayr, H. (2013): "Multiplex detection of antibiotic resistance genes using padlock probes". In: *Diagnostic Microbiology and Infectious Disease* 77 (2), pp. 118-125.

Barsoukov, E. and Macdonald, J. R. (Ed.) (2005): "Impedance Spectroscopy: Theory, Experiment, and Applications". 2nd Edition: *Wiley-VCH-Interscience*.

Bendich, J.A. and Drlica, K. (2000): "Prokaryotic and eukaryotic chromosomes: what's the difference". In: *BioEssays* 22, pp. 481-486.

Budkevich, T. V.; El'skaya, A. V. and Nierhaus, K. H. (2008): "Features of 80S mammalian ribosome and its subunits". In: *Nucleic Acids Research* 36 (14), pp. 4736-4744.

Bush, K. and Jacoby, A. G. (2010): "Updated Functional Classification of β -lactamases". In: *Antimicrobial Agents and Chemotherapy* 54 (3), pp. 969-976.

Bush, K.; Jacoby, A. G. and Meideiros, A.A. (1995): "A Functional Classification Scheme for β -Lactamases and Its Correlation with Molecular Structure". In: *Antimicrobial Agents and Chemotherapy* 39 (6), pp. 1211-1233.

Byarugaba, D.K (2004): "Antimicrobial resistance in developing countries and responsible risk factors". In: *International Journal of Antimicrobial Agents* 24 (2), pp. 105-110.

Byarugaba, D. K. (2010): "Mechanisms of Antimicrobial Resistance". In: Sosa, A.J.; Byarugaba, D.K; Amabile-Cuevas, F.C.; Hsueh, P.R.; Kariuki, S. and Okeke, N.I. (Ed.): "Antimicrobial Resistance in Developing Countries". *Springer*, pp. 15-26.

Cairns, J.; Overbaugh, J. and Miller, S. (1988): "The origin of mutants". In: *Nature America* 335, pp. 142-145.

Clermont, O.; Bonacorsi, S. and Bingen, E. (2000): "Rapid and Simple Determination of the Escherichia coli Phylogenetic Group". In: *Applied and Environmental Microbiology* 66 (10), pp. 4555-4558.

Daniels, S.J. and Pourmand, N. (2007): "Label-Free Impedance Biosensors: Opportunities and Challenges". In: *Electroanalysis* 19 (12), pp. 1239-1257.

Dean, B.F.; Nelson, R.J.; Giesler, L.T. and Lasken, S.R. (2001): "Rapid Amplification of Plasmid and Phage DNA Using Phi29 DNA Polymerase and Multiply-Primed Rolling Circle Amplification". In: *Genome Research* 11, pp. 1095-1099.

Diekema, J. D. and Jones, N. R. (2001): "Oxazolidinone antibiotics". In: *The Lancet* 358, pp. 1975-1982.

Dzidic, S.; Suskovic, J. and Kos, B. (2008): "Antibiotic Resistance Mechanisms in Bacteria: Biochemical and Genetic Aspects". In: *Food Technology and Biotechnology* 46 (1), pp. 11-21.

eMedExpert (2013): "Antibiotics: Types and Side Effects". <http://www.emedexpert.com/classes/antibiotics.shtml> (May 13, 2014).

Ertuğrul, D.H. and Uygun, O.Z. (2013): "Impedimetric Biosensors for Label-Free and Enzymless Detection". In: Dr. Rinken, T. (Ed.): "State of the Art in Biosensors - General Aspects". *InTech*, pp. 179-196.

Fluit, A. C.; Visser, M. R. and Schmitz, F. J. (2001): "Molecular Detection of Antimicrobial Resistance". In: *Clinical Microbiology Reviews* 14 (4), pp. 836-871.

Gamry, Instruments (2010): "Basics of Electrochemical Impedance Spectroscopy". In: *Application Note Rev. 1.0*, pp. 1-17. <http://www.gamry.com/application-notes/basics-of-electrochemical-impedance-spectroscopy/> (January 05, 2014).

Giedraitiene, A.; Vitkauskienė, A.; Naginiene, R. and Pavilonis, A. (2011): "Antibiotic Resistance Mechanism of Clinically Important Bacteria". In: *Medicina (Kaunas)* 47 (3), pp. 137-146.

Gill, P. and Ghaemi, A. (2008): "Nucleic Acid Isothermal Amplification Technologies—A Review". In: *Nucleosides, Nucleotides and Nucleic Acids* 27 (3), pp. 224-243.

Goddemeier, C. (2006): "Penicillin. Vor 125 Jahren wurde der Arzt und Forscher geboren". In: *Deutsches Ärzteblatt* 103 (36), p. A2286.

Gomadam, M.P. and Weidner, W.J. (2005): "Analysis of electrochemical impedance spectroscopy in proton exchange membrane fuel cells". In: *International Journal of Energy Research* 29, pp. 1133-1151.

Griffiths, A.J.F.; Miller, J.H.; Suzuki, D.T.; *et al.* (Ed.) (2000): "An Introduction to Genetic Analysis, Gene Transfer in Bacteria and Their Viruses". 7th Edition: *W. H. Freeman*, pp. 155-165.

Hamdy, S.A.; El-Shenawy, E. and El-Bitar, T. (2006): "Electrochemical Impedance Spectroscopy Study of the Corrosion Behavior of Some Niobium Bearing Stainless Steels in 3.5% NaCl". In: *International Journal of Electrochemical Science* 1, pp. 171-180.

Hooper, C. D. (1999): "Mechanisms of fluoroquinolone resistance". In: *Drug Resistance Updates* 2, pp. 38-55.

Inzelt, G. (2007): "Charge Transport in Conducting Polymer Film Electrodes". In: *Chemical and Biochemical Engineering Quarterly* 21 (1), pp. 1-14.

Jiang, D.; Xiang, G.; Wu, X.; Liu, C, Liu, F. and Pu, X. (2012): "A Real-time Resistance Measurement for DNA Amplification and Detection". In: *International Journal of Electrochemical Science* 7, pp. 5273-5285.

Kay, E.; Vogel, T. M.; Bertolla, F.; Nalin, R. and Simonet, P. (2002): "In Situ Transfer of Antibiotic Resistance Genes from Transgenic (Transplastomic) Tobacco Plants to Bacteria". In: *Applied and Environmental Microbiology* 68 (7), pp. 3345-3351.

Keen, E. C. (2012): "Phage Therapy: Concept to Cure". In: *Frontiers in Microbiology* 3 (238), pp. 1-3.

Kiiru, J.; Kariuki, S.; Goddeeris, M. B. and Butaye, P. (2012): "Analysis of beta-lactamase phenotypes and carriage of selected beta-lactamase genes among *Escherichia coli* strains obtained from Kenyan patients during an 18-year period". In: *Biomedcentral (BMC) Microbiology* 12, pp. 155.

Kodzius, R.; Xiao, K.; Wu, J.; Yi, X.; Gong, X.; Foulds, G.I. and Wen, W. (2012): "Inhibitory effect of common microfluidic materials on PCR outcome". In: *Sensors and Actuators B* 161, pp. 349-358.

Kong, K.F.; Schneper, L. and Mathee, K. (2010): "Beta-lactam Antibiotics: From Antibiotics to Resistance and Bacteriology". In: *Acta pathologica, microbiologica, et immunologica Scandinavica (APMIS)* 118 (1), pp. 1-36.

- Koonin, V. E.; Makarova, S. K. and Aravind, L. (2001): "Horizontal Gene Transfer in Prokaryotes: Quantification and Classification". In: *Annual Review of Microbiology* 55, pp. 709-742.
- Kubista, M.; Andrade, J. M.; Bengtsson, M.; Forootan, A.; Jonák, J.; Lind, K. et al. (2006): "The real-time polymerase chain reaction". In: *Molecular Aspects of Medicine* 27 (2-3), pp. 95-125.
- Lasia, A. (1999): "Electrochemical Impedance Spectroscopy and its Applications, Modern Aspects of Electrochemistry". In: *Kluwer Academic/Plenum Publishers* 32, pp. 143-248.
- Löwdin, P.O. (1963): "Proton tunneling in DNA and its biological implications". In: *Reviews of Modern Physics* 3, pp. 724-732.
- Lvovich, F.V. (Ed.) (2012): "Impedance Spectroscopy: Applications to Electrochemical and Dielectric Phenomena". *Wiley-VCH*.
- Ma, H.; Wallbank, W.R.R.; Chaji, R.; Li, J.; Suzuki, Y.; Jiggins, C. and Nathan A. (2013): "An impedance-based integrated biosensor for suspended DNA characterization". In: *Scientific Reports* 3: 2730, pp. 1-7.
- Macdonald, J. R. (1992): "Impedance Spectroscopy". In: *Annals of Biomedical Engineering* 20, pp. 289-305.
- Madigan, T.M.; Martinko, M.J.; Dunlap, V.P. and Clark, P.D. (Ed.) (2009): "Brock-Biology of microorganisms". 12th Edition: *Pearson Education*, pp. 793-809.
- Majiduddin, F.K.; Materon, I.C. and Palzkill, T.G. (2002): "Molecular analysis of beta-lactamase structure and function". In: *International Journal of Medical Microbiology* 292, pp. 127-137.
- Maloy, S. (July 15, 2002). "Polymerase Chain Reaction" <http://www.sci.sdsu.edu/~smaloy/MicrobialGenetics/topics/in-vitro-genetics/PCR.html>. San Diego State University (November 18, 2013).
- Mothershed, E. A. and Whitney, A. M. (2006): "Nucleic acid-based methods for the detection of bacterial pathogens: Present and future considerations for the clinical laboratory". In: *Clinica Chimica Acta* 363 (1-2), pp. 206-220.
- Nasehi, L.; Shahcheraghi, F.; Nikbin, S. V. and Nematzadeh, S. (2010): "PER, CTX-M, TEM and SHV Beta-lactamases in clinical isolates of *Klebsiella pneumoniae* isolated from Tehran, Iran". In: *Iranian Journal of Basic Medical Sciences* 3, pp. 111-118.

Nilsson, M.; Dahl, F.; Larsson, C.; Gullberg, M. and Stenberg, J. (2006): "Analyzing genes using closing and replicating circles". In: *Trends in Biotechnology* 24 (2), pp. 83-88.

Paterson, D.L. and Bonomo, R.A. (2005): "Extended-Spectrum β -Lactamases: a Clinical Update". In: *Clinical Microbiology Reviews* 18 (4), pp. 657-686.

Pourmand, N.; Karhanek, M.; Persson, H.J.H; Webb, D.C.; Lee, H.T.; Zahradníková, A. and Davis, W.R. (2006): "Direct electrical detection of DNA synthesis". In: *Proceedings of the National Academy of Sciences (PNAS)* 103 (17), pp. 6466-6470.

Rollins, M.D. (2004). "BSCI 223 - General Microbiology"
<http://www.life.umd.edu/classroom/bsci424/BSCI223WebSiteFiles/ProkaryoticvsEukaryotic.htm>. University of Maryland (April 01, 2014).

Ruggy, G. (1945): "Reviews Papers: A Review of the Problems of Sulfonamide Chemotherapy". In: *Ohio Journal of Science* 45 (3), pp. 115-124.

Rychlik, W.; Spencer, W.J. and Rhoads, R.E. (1990): "Optimization of the annealing temperature for DNA amplification in vitro". In: *Nucleic Acids Research* 21, pp. 6409-6412.

Saiki, R.; Scharf, S.; Faloona, F.; Mullis, K.; Horn, G.; Erlich, H. and Arnheim, N. (1985): "Enzymatic Amplification of beta-Globin Genomic Sequences and Restriction Site Analysis for Diagnosis of Sickle Cell Anemia". In: *Science* 4732, pp. 1350-1354.

Schmid, D. R (Ed.) (2006): "Taschenatlas der Biotechnologie und Gentechnik". 2. Auflage: *WILEY-VCH*, pp. 34-53.

Tenson, T.; Lovmar, M. and Ehrenberg, M. (2003): "The mechanism of Action of Macrolides, Lincosamides and Streptogramin B Reveals the Nascent Peptide Exit Path in the Ribosome". In: *Journal of Molecular Biology* 330 (5), pp. 1005-1014.

Todar, K. (2009): "Bacterial Resistance to Antibiotics"
<http://textbookofbacteriology.net/themicrobialworld/bactresanti.html>. University of Wisconsin-Madison. (November 11, 2013).

Van Bambeke, F.; Van Laethem, Y.; Courvalin, P. and Tulkens, M.P. (2004): "Glycopeptide Antibiotics from Conventional molecules to New Derivatives". In: *Drugs* 64 (9), pp. 913-936.

VITEK2 technology (2008) © bioMérieux Inc. Customer Edition. <http://www.biomerieux-usa.com/upload/VITEK-Bus-Module-1-Antibiotic-Classification-and-Modes-of-Action-1.pdf> (March 30, 2014).

Walsh, C. (2000): "Molecular mechanism that confer antibacterial drug resistance". In: *Nature* 406, pp. 775-781.

Walther-Rasmussen, J. and Hoiby, N. (2006): "OXA-type carbapenemases". In: *Journal of Antimicrobial Chemotherapy* 57 (3), pp. 373-383.

Walther-Rasmussen, J. and Hoiby, N. (2007): "Class A carbapenemases". In: *Journal of Antimicrobial Chemotherapy* 60, pp. 470-482.

Yusof, M.; Mei Yi, D.C.; Enhui, J.L.; Mohd Noor, N.; Wan Ab Razak, W. and Saad Abdul Rahim, A. (2011): "An illustrated review on penicillin and cephalosporin: An instant study guide for pharmacy students". In: *WebmedCentral Pharmaceutical Sciences* 2 (12): WMC002776, pp. 1-11.

Zanoli, L. and Spoto, G. (2013): "Isothermal Amplification Methods for the Detection of Nucleic Acids in Microfluidic Devices". In: *Biosensors* 3 (1), pp. 18-43.

Zhang, Y. (2008): "Mechanism of Antibiotic Resistance in the microbial world". In: *Clinical Pharmacology & Therapeutics* 82, pp. 595-600.

5.2 List of tables:

Table 1: Semi-synthetic analogs of tetracycline antibiotics.....	- 5 -
Table 2: 33 Important clinical β -lactamases	- 12 -
Table 3: Common electrical circuit elements.....	- 23 -
Table 4: Phosphorylation protocol of the padlock probes.....	- 36 -
Table 5: RCA protocol	- 37 -
Table 6: Parameters of the four different IDEs structures	- 40 -
Table 7: Results of Δ ABS-Z at 184, 295 and 472 kHz.	- 56 -

5.3 List of figures:

Figure 1: Illustration of a microbial cell.....	- 3 -
Figure 2: Penicillin mechanism of action.....	- 4 -
Figure 3: Analogs of tetracycline	- 4 -
Figure 4: Illustration of erythromycin	- 5 -
Figure 5: Illustration of Streptomycin	- 6 -
	- 67 -

Figure 6: Illustration of ciprofloxacin	- 6 -
Figure 7: Illustration of vancomycin	- 7 -
Figure 8: Illustration of clindamycin.....	- 7 -
Figure 9: Illustration of linezolid, also called zyvox.....	- 8 -
Figure 10: Illustration of sulfisoxazole, also known as sulfafurazole.....	- 8 -
Figure 11: Mechanism of PCR.....	- 15 -
Figure 12: Schematic illustration of the four different elements on a padlock probe	- 17 -
Figure 13: Schematic illustration of padlock probes through ligation process	- 18 -
Figure 14: Mechanism of RCA/RCR	- 19 -
Figure 15: Sinusoidal current response in a linear system	- 22 -
Figure 16: The impedance plotted using rectangular and polar coordinates.....	- 23 -
Figure 17: (A) Impedance in series and (B) in parallel.....	- 24 -
Figure 18: Simplified ECM - $[(R-2C_{\text{coupled}}) C_{\text{parasitic}}]$	- 25 -
Figure 19: LOG-LOG representation of ABS-Z vs. frequency for three different values of R- Analyte ($R_1 > R_2 > R_3$).	- 27 -
Figure 20: ABS-Z, phase, $\text{Re}(Z)$ and $\text{ABS-Im}(Z)$ for $C_{\text{coupled}} = 6 \text{ nF}$, $C_{\text{parasitic}} = 200 \text{ pF}$ and R- Analyte = 10 kOhm vs. frequency ($100 \text{ Hz} - 1 \text{ MHz}$).....	- 28 -
Figure 21: ABS-Z and phase for different coupling and parasitic capacitances at a value of R- Analyte = 10 kOhm vs. frequency ($100 \text{ Hz} - 1 \text{ MHz}$).....	- 29 -
Figure 22: Position of the switches by an Open-Short-correction	- 34 -
Figure 23: Image of Biosensor_Virus provided by Infineon, Villach.....	- 40 -
Figure 24: Image of a filled chip, taken through the eyepiece of a microscope	- 41 -
Figure 25: ABS-Z vs. frequency – Biosensor_Virus_Infineon – structure V1	- 42 -
Figure 26: Two images of the 2 ml sensor.	- 43 -
Figure 27: ABS-Z vs. frequency of differently concentrated KCl solutions in a 2 ml reaction tube	- 44 -
Figure 28: (A) Image and (B) schematic overview of the final sensor, called Biosensor_RCA_bla_AIT	- 45 -

Figure 29: ABS-Z vs. frequency – Biosensor_RCA_bla_AIT – of differently concentrated KCl solutions.....	- 46 -
Figure 30: Re(Z) vs. frequency – Biosensor_RCA_bla_AIT – of differently concentrated KCl solutions	- 47 -
Figure 31: Phase vs. frequency – Biosensor_RCA_bla_AIT – of differently concentrated KCl solutions	- 48 -
Figure 32: Phase vs. frequency – Biosensor_RCA_bla_AIT – of 100 mM KCl solution at different filling levels (= one capillary at each wire).	- 49 -
Figure 33: ABS-Z vs. frequency – Biosensor_RCA_bla_AIT – of 100 mM KCl solution at different filling levels (= one capillary at each wire)	- 50 -
Figure 34: Phase vs. frequency – Biosensor_RCA_bla_AIT – of 100 mM KCl solution at different filling levels (= two capillaries at each wire)	- 51 -
Figure 35: ABS-Z vs. frequency – Biosensor_RCA_bla_AIT – of 100 mM KCl solution at different filling levels (= two capillaries at each wire)	- 51 -
Figure 36: ABS-Z vs. frequency (10 kHz – 1 MHz) of phi29 buffer at different temperatures (RT, 37 °C and 65 °C).....	- 52 -
Figure 37: ABS-Z vs. frequency (100 kHz – 960 kHz) of a positive control.....	- 53 -
Figure 38: ABS-Z vs. frequency (100 kHz – 960 kHz) of a negative control	- 54 -
Figure 39: Time dependence of ABS-Z of both three positive (Positive_1-3) and negative (Negative_1-3) controls at 184 kHz	- 55 -
Figure 40: Time dependence of ABS-Z of both three positive (Positive_1-3) and negative (Negative_1-3) controls at 472 kHz	- 55 -
Figure 41: Image of agarose gel electrophoresis.....	- 57 -
Figure 42: Time dependence of ABS-Z of both two positive (Positive_30°C_1-2) and negative controls (Negative_30°C_1-2) at 472 kHz (30 °C)	- 58 -
Figure 43: Δ ABS-Z at 472 kHz vs. initial target concentration (C_0) calculated on the 1 st RCA approach	- 59 -
Figure 44: Schematic overview of a sensor based on passivated planar electrodes, which are connected to each other by a microfluidic.	- 61 -

5.4 MATLAB - Source code of the (R-2C_{coupled})/C_{parasitic} - ECM:

```
%% Simplified Equivalent circuit Model - ECM - Calculation + Data export
%
% ECM see figure 18
%
% Made by: Konrad Kainz
% Date: 13.05.2014
% Copyright: Austrian Institute of Technology (AIT)
%
%% Parameter (fix):
%
Cp1=6e-9;           % Capacitance of Passivation Layer - Ccoupled
Cp2=2e-12;          % Parasitic capacity - Cparasitic
R=[18.2e6,10000,100]; % Resistor-Range [Ohms]
%                  % ~18.2e6 = dH2O; ~10000 = 1mMKCl; ~100 = 100mMKCl
f=logspace(2,6,100); % Frequency range [Hz]
w=2*pi.*f;          % w (=omega)
%
%% Calculation - ECM:
ZII=0;
for n=1:length(R);
    for m=1:length(f);
        Z1buff=1/(1i*w(m)*Cp2);
        Z2buff=((R(n)+(1./(1i*pi*f(m)*Cp1))));
        Z3buff=Z1buff*Z2buff;
        Z4buff=Z1buff+Z2buff;
        ZII(n,m)=Z3buff/Z4buff;
    end
end
%
%% Data export:
ResultBuffer=f';
% %
for n=1:length(R);
    ABSbuffer=abs(ZII(n,:));
    ANGLEbuffer=angle(ZII(n,:))/pi*180;
    REbuffer=real(ZII(n,:));
    IMbuffer=imag(ZII(n,:));
    ResultBuffer=[ResultBuffer,ABSbuffer',ANGLEbuffer',REbuffer',IMbuffer'];
end
% %
dlmwrite('Title',ResultBuffer,'delimiter','t','newline','pc');
%
%% Plotten - ZII:
figure;
hold on
for n=1:length(R);
    ABSZIIbuffer=abs(ZII(n,:));
    plot(f,ABSZIIbuffer,'-xr');
    axis tight;
end
- 70 -
```

```

        xlabel('Frequency [Hz]');
        ylabel('ABS-Z [Ohms]');
        ht=title('ABS-Z');
        set(ht,'FontWeight','bold');
        set(gca,'yscale','log','xscale','log');
        grid;
    end
    %
    figure;
    hold on
    for n=1:length(R);
        ABSREZIIbuffer=abs(real(ZII(n,:)));
        plot(f,ABSREZIIbuffer,'-xr');
        axis tight;
        xlabel('Frequency [Hz]');
        ylabel('ABS-Real-Z [Ohms]');
        ht=title('ABS-Real-Z');
        set(ht,'FontWeight','bold');
        set(gca,'yscale','log','xscale','log');
        grid;
    end
    %
    figure;
    hold on
    for n=1:length(R);
        ABSIMZIIbuffer=abs(imag(ZII(n,:)));
        plot(f,ABSIMZIIbuffer,'-xr');
        axis tight;
        xlabel('Frequency [Hz]');
        ylabel('ABS-Im-Z [Ohms]');
        ht=title('ABS-Im-Z');
        set(ht,'FontWeight','bold');
        set(gca,'yscale','log','xscale','log');
        grid;
    end
    %
    figure;
    hold on
    for n=1:length(R);
        ANGLEZIIbuffer=angle(ZII(n,:))/pi*180;
        plot(f,ANGLEZIIbuffer,'-xr');
        axis tight;
        xlabel('Frequency [Hz]');
        ylabel('Phase [°]');
        ht=title('Angle');
        set(ht,'FontWeight','bold');
        set(gca,'xscale','log');
        grid;
    end
    %

```


6 Curriculum Vitae:

Name: Konrad Kainz
E-Mail: konrad.kainz@gmx.at
Birth date/place: 15.08.1988 / Vienna, Austria

Education:

Since 03/2013 Vienna University of Technology (Material chemistry)
Desired degree: Master of Science
10/2007 - 03/2013 Vienna University of Technology (Technical chemistry)
Degree: Bachelor of Science
Title of the Bachelor thesis: Loop-mediated isothermal Amplification
09/1998 - 06/2006 Bundesrealgymnasium Wien XVIII, Schopenhauerstrasse 49
Degree: Matura (Final Exam)

Work Experience:

09/2013 – 04/2014 Research Associate (Master's thesis) at the Department: Health & Environment (Business Unit: Molecular Diagnostic) – AIT – TechGate Vienna
10/2010 - 06/2011 Research Associate at the Department: Health & Environment (Business Unit: Bioresources) – AIT – Seibersdorf and Tulln
07/ 2010 - 09/2010 Practicant student at the Department: Health & Environment (Business Unit: Bioresources) – AIT – Seibersdorf
01/2009 - 08/2009 Professional detective assistant at K&M BLEYER GMBH
– Credit & detective agency
07/2004 - 08/2004 Internship at the company K&M BLEYER GMBH
– Credit & detective agency